

# EXTREMILE SCALAR-ON-FUNCTION REGRESSION WITH APPLICATION TO CLIMATE SCENARIOS

BY MARIA LAURA BATTAGLIOLA<sup>1,a</sup> AND MARTIN BLADT<sup>2,b</sup>

<sup>1</sup> *INSTITUTE OF MATHEMATICS, ÉCOLE POLYTECHNIQUE FÉDÉRALE DE LAUSANNE, <sup>a</sup>LAURA.BATTAGLIOLA@EPFL.CH*

<sup>2</sup> *DEPARTMENT OF MATHEMATICAL SCIENCES, UNIVERSITY OF COPENHAGEN, <sup>b</sup>MARTINBLADT@MATH.KU.DK*

Extremiles provide a generalization of quantiles which are not only robust, but also have an intrinsic link with extreme value theory. This paper introduces an extremile regression model tailored for functional covariate spaces. The estimation procedure turns out to be a weighted version of local linear scalar-on-function regression, where now a double kernel approach plays a crucial role. Asymptotic expressions for the bias and variance are established, applicable to both decreasing bandwidth sequences and automatically selected bandwidths. The methodology is then investigated in detail through a simulation study. Furthermore, we highlight the applicability of the model through the analysis of data sourced from the CH2018 Swiss climate scenarios project, offering insights into its ability to serve as a modern tool to quantify climate behaviour.

**1. Introduction.** Changes in climate pose an ever more important threat to global ecosystems and human societies, manifesting among other things through increased frequency and intensity of extreme weather events. Understanding and forecasting such events is thus a crucial task due to the environmental and socioeconomic impacts they carry. In statistics, given the nature of the phenomena characterizing changes in climate, it is only natural to study these under the lens of Extreme Value Theory (EVT). In particular, EVT offers established tools to detect and analyze rare but highly consequential events, providing insight into catastrophic events. Such insight can in turn serve a crucial role for effective risk management and mitigation/adaptation strategies for the emerging risks we face.

Quantile regression (Koenker and Bassett, 1978) is a classic statistical tool that allows for the estimation and prediction of quantiles of the responses conditional on the covariates. Newey and Powell (1987) defined another measure of extremes, namely expectiles. However, they do not enjoy a straightforward interpretability as quantiles, and efforts have been made to link expectiles to generalized quantiles (see for instance Jones (1994) and Bellini et al. (2014)). On the other hand, extremiles, first introduced by Daouia, Gijbels and Stupfler (2019), differ from quantiles as they do not revolve around the empirical conditional quantile function, i.e., the inverse of the cumulative distribution function (CDF), of the responses. Rather, they represent the expected maximum or minimum of independent realizations from the conditional distribution of the responses given the covariates. This natural interpretation brings extremiles one conceptual step closer to interpretability in terms of EVT. In particular, the number of realizations increases as the extremile level becomes more extreme, i.e., close to 0 or 1. This feature makes them more robust than quantiles, as higher (or lower) order quantiles become more difficult to estimate as the available data becomes scarcer.

Another characteristic of climate phenomena is their complexity, largely due to their continuous nature over time and space. Given this intrinsic feature, other statistical disciplines have classically dominated their analysis. For instance, Functional Data Analysis (FDA) has

---

*Keywords and phrases:* Extremile regression, Functional data analysis, Bandwidth selection, Climate change.

been the staple framework to represent them in a realistic manner, allowing them to be treated as continuous functions (see for instance [Zhang et al. \(2011\)](#), [Bonner, Newlands and Heckman \(2014\)](#), [Fraiman et al. \(2014\)](#), [Suhaila and Yusop \(2017\)](#), [Tapia et al. \(2022\)](#), [Villani, Romano and Mateu \(2024\)](#)). Compared to multivariate data, functional data have the additional intricacies of being infinite dimensional as well as not being exchangeable over the functional coordinate they smoothly vary over. Thus, development of targeted frameworks and methodologies is imperative to work with such data. In particular, recent advances have been dedicated to the integration of EVT and FDA. Among those, scalar-on-function quantile regression ([Guo et al., 2015](#); [Yu, Kong and Mizera, 2016](#); [Li et al., 2022](#)) and scalar-on-function expectile regression ([Mohammedi, Bouzebda and Laksaci, 2021](#); [Rachdi, Laksaci and Al-Kandari](#)) have recently gained popularity. Notably, [Girard, Stupfler and Usseglio-Carleve \(2022\)](#) and [Di Bernardino, Laloë and Pakzad \(2024\)](#) focused on the estimation of extreme conditional expectiles when covariates are functions.

In this paper we propose a state-of-the-art statistical model for effective analysis of climate data. However, we do so by straying away from functional regression in the classical sense. Instead, with an interpretable and robust model, we focus on extending extremile regression ([Daouia, Gijbels and Stupfler, 2022](#)) to when covariates are functional. In practical terms, we achieve this by considering a weighted version of the scalar-on-function local linear regression ([Baïllo and Grané, 2009](#); [J. Barrientos-Marin and Vieu, 2010](#); [Boj, Delicado and Fortiana, 2010](#)) studied by [Ferraty and Nagy \(2021\)](#). In particular, the weights depend on the extremile level considered as well as the estimate of the conditional CDF. We obtain such an estimate via Nadaraya-Watson-type estimators whose kernel bandwidths are chosen according to the procedure of [Chagny and Roche \(2014\)](#). The methodology introduced allows us to investigate the effects of climate change in Switzerland by studying two different simulated scenarios reflecting the climatic conditions in the middle of the current century. Notably, one scenario assumes climate mitigation measures were adopted from the present day, and the other assumes no action was taken to combat climate change. This data was produced within the CH2018 climate scenarios for Switzerland project ([CH2018, 2018](#)). We compare estimated and predicted extremes of low levels of monthly average relative humidity and those of high levels of monthly mean temperature at 42 different Swiss weather stations across the two scenarios between May and September. Our goal is to determine whether future summers will be drier and/or warmer and, if so, by how much. The measure here is in terms of extremiles, which are linked to maxima of samples of varying sizes. From our analysis, among other things, we may conclude that humidity will indeed decrease and temperatures will increase in the future. The magnitude of such climate risks crucially depends on whether climate measures are adopted as soon as possible.

This manuscript is structured as follows: in Section 2 we provide an overview of the fundamental concepts of extremile regression and mean local linear scalar-on-function regression. Such mathematical tools are used in Section 3 to outline the methodological framework of our work. In particular, we provide rates of convergence of the asymptotic bias and variance of the conditional extremile estimator for scalar-on-function models, and the proofs may be found in appendix A. In Section 4 we study the performance of the proposed methodology in a simulation study. Section 5 is dedicated to the thorough analysis of climate risks based on the CH2018 climate scenarios for Switzerland project. Finally, we summarize our findings and discuss possible further developments in Section 6. Additional results corresponding to Sections 4 and 5 can be found in appendix B.

**2. Preliminaries.** This section provides some preliminaries on conditional extremiles and local linear regression with functional covariates. Its primary aim is to provide notation and intuition for the construction of our main model, which has elements of both approaches.

2.1. *Extremile regression for multivariate covariates.* Consider the estimation of conditional extremiles on non-functional covariates, cf. [Daouia, Gijbels and Stupfler \(2022\)](#). Specifically, consider the random variables  $Y \in \mathbb{R}$  and  $X \in \mathbb{R}^d$ , and call

$$F(y|x) = \mathbb{P}(Y \leq y|X = x)$$

the conditional CDF of  $Y$  given  $X = x$ . Moreover, assume that  $\mathbb{E}[|Y||X = x] < \infty$ . For any fixed  $\tau \in (0, 1)$ , the *conditional extremile of order  $\tau$*  of  $Y$  given  $X = x$  is defined as

$$(1) \quad \xi_\tau(x) = \arg \min_{\theta \in \mathbb{R}} \mathbb{E}[J_\tau(F(Y|X)) \cdot (|Y - \theta|^2 - |Y|^2)|X = x],$$

where  $J_\tau(\cdot) = K'_\tau(\cdot)$ , with

$$K_\tau(t) = \begin{cases} 1 - (1 - t)^{s(\tau)} & \text{if } \tau \in (0, 1/2] \\ t^{r(\tau)} & \text{if } \tau \in [1/2, 1) \end{cases}$$

for  $t \in [0, 1]$ , and  $r(\tau) = s(1 - \tau) = \log(1/2)/\log(\tau)$ . Moreover, we have that

$$(2) \quad \xi_\tau(x) = \mathbb{E}[Y J_\tau(F(Y|X))|X = x].$$

An alternative representation, first given by [Daouia, Gijbels and Stupfler \(2019\)](#) for the marginal extremile and extended to the conditional extremile (2) by [Daouia, Gijbels and Stupfler \(2022\)](#), is

$$(3) \quad \xi_\tau(x) = \begin{cases} \mathbb{E} \left[ \min \left( Y_1^x, \dots, Y_{\lfloor s(\tau) \rfloor}^x \right) \right] & \text{if } \tau \in (0, 1/2] \\ \mathbb{E} \left[ \max \left( Y_1^x, \dots, Y_{\lfloor r(\tau) \rfloor}^x \right) \right] & \text{if } \tau \in [1/2, 1) \end{cases}$$

where  $Y_1^x, \dots, Y_{\lfloor s(\tau) \rfloor}^x$  and  $Y_1^x, \dots, Y_{\lfloor r(\tau) \rfloor}^x$  are  $\lfloor s(\tau) \rfloor$  and  $\lfloor r(\tau) \rfloor$  independent and identically distributed copies drawn from the conditional distribution of  $Y$  given  $X = x$ . As  $\tau \uparrow 1$ , and thus  $r(\tau) \rightarrow \infty$ , the number of copies of  $Y$  increases, and so does the average of their maximum. In a symmetrical way, when  $\tau \downarrow 0$  and  $s(\tau) \rightarrow \infty$ ,  $\xi_\tau(x)$  decreases.

Consider now an independent and identically distributed sample  $(Y_i, X_i)_{i=1, \dots, n}$ . A local linear approximation to (1) is obtained for any  $h > 0$  by

$$(4) \quad (\hat{\alpha}_\tau, \hat{\beta}_\tau) = \arg \min_{\alpha, \beta \in \mathbb{R}} \sum_{i=1}^n J_\tau(\hat{F}(Y_i|x)) \{Y_i - \alpha - \beta(x - X_i)\}^2 L\left(\frac{x - X_i}{h}\right),$$

where  $\hat{F}(\cdot|x)$  is any uniformly consistent estimator of  $F(\cdot|x)$ , and  $\hat{\alpha}_\tau$  is the estimator of  $\xi_\tau$ . Notice that (4) is a weighted least squares problem solving the locally linearized check function  $\rho_\tau(v) = v(\tau - 1(v \leq 0))$ , using kernel  $L$  with bandwidth sequence  $h = h_n$  such that  $h_n \rightarrow 0$  as  $n \rightarrow \infty$ . The solutions to (4) turn out to have a closed form, and [Daouia, Gijbels and Stupfler \(2022\)](#) showed asymptotic unbiasedness and normality of the extremile estimator, under further regularity conditions.

2.2. *Local linear scalar-on-function regression.* Consider now random variables  $Y \in \mathbb{R}$  and a random element  $X(\cdot) \in E$ , where  $(E, d)$  is a semi-metric space with semi-metric  $d$ . The choice of  $d$  depends on the problem one aims at solving, as is explained in detail in [Ferraty and Vieu, 2006](#), Chapter 3). However, in most applications  $E = L^2(\mathcal{S})$ , where  $\mathcal{S} \subset \mathbb{R}$ , and  $d^2(X_1, X_2) = \int_{\mathcal{S}} (X_1(s) - X_2(s))^2 ds$  for any  $X_1(\cdot), X_2(\cdot) \in E$ ; we also adopt such functional space. Hence,  $\langle X_1, X_2 \rangle = \int_{\mathcal{S}} X_1(s) X_2(s) ds$  and  $\|X_1\|^2 = \int_{\mathcal{S}} X_1^2(s) ds$ .

A local linear mean regression model for functional regressors and scalar responses was proposed in [Ferraty and Nagy \(2021\)](#). Such type of regression is nonparametric and models a linear relationship between response and covariates in a subset of  $E$ . In particular, given

$x(\cdot) \in E$  and independent and identically distributed observations  $(Y_i, X_i(\cdot))_{i=1, \dots, n}$ , the scalar-on-function local linear mean regression model around  $x$  is given by

$$(5) \quad (\hat{\alpha}, \hat{\beta}) = \arg \min_{\alpha \in \mathbb{R}, \beta \in L^2(\mathcal{S})} \sum_{i=1}^n \{Y_i - \alpha - \langle \beta, x - X_i \rangle\}^2 L\left(\frac{\|x - X_i\|}{h}\right).$$

The minimizers in (5) correspond to the estimators of the local linear mean and its functional derivative in  $x(\cdot)$ , namely  $\hat{\alpha}$  and  $\hat{\beta}$ , respectively. Notice that, under the assumption that the first order Taylor expansion of the estimator around  $x(\cdot)$  is valid, the functional derivative is the local linear approximation of the mean regression operator evaluated in a neighborhood of  $x$ . Hence, analysing the properties of  $\hat{\beta}$  leads to a better understanding of the robustness of the estimator  $\hat{\alpha}$ . Notice that even though  $\hat{\alpha}, \hat{\beta}$  depend on  $x(\cdot), h$  and  $n$ , we avoid specifying this dependence in the notation for ease of exposition.

To reduce the infinite dimensional problem in (5), one can approximate unknown functional coefficient  $\beta$  with a truncated representation involving known basis functions. More specifically, one may take

$$(6) \quad \beta \approx \mathcal{P}_K(\beta) = \sum_{k=1}^K b_k \phi_k,$$

where  $\mathcal{P}_K(\cdot)$  indicates the projection onto subspace  $\mathcal{F}^K$  of  $L^2(\mathcal{S})$ , and  $\{\phi_k(\cdot)\}_{k=1}^K$  are  $K$  orthonormal basis functions spanning  $\mathcal{F}^K$ , with  $b_k = \langle \phi_k, \beta \rangle$ . We can now consider finite dimensional version of (5) which only relies on scalar coefficients, namely

$$(7) \quad (\hat{\alpha}, \hat{b}_1, \dots, \hat{b}_K) = \arg \min_{\alpha, b_1, \dots, b_K \in \mathbb{R}} \sum_{i=1}^n \left\{ Y_i - \alpha - \sum_{k=1}^K b_k \langle \phi_k, x - X_i \rangle \right\}^2 L\left(\frac{\|x - X_i\|}{h}\right).$$

**3. Extremile scalar-on-function regression.** In this section we introduce our model, which essentially combines the methodologies presented in Section 2, defining a framework for extremile scalar-on-function regression. In particular, we derive the closed form of the extremile estimator of order  $\tau$ , and we study some of its basic asymptotic properties through techniques akin to scalar-on-function regression.

**3.1. Setting and problem formulation.** Given the random variable  $Y \in \mathbb{R}$  and random element  $X(\cdot) \in E$ , we use the same notation as in (2) to write the conditional extremile, namely  $\xi_\tau(x) = \mathbb{E}[Y J_\tau(F(Y|X)) | X = x]$ , where  $F(\cdot|x)$  the conditional CDF of the scalar response  $Y$  given the functional covariate  $X = x$ . Notice that the expression (3) carries over to this framework as well, with  $Y_1^x, \dots, Y_{\lfloor s(\tau) \rfloor}^x$  and  $Y_1^x, \dots, Y_{\lfloor r(\tau) \rfloor}^x$  independent copies from the conditional distribution of  $Y$  given the functional  $X = x$ .

Consider now independent and identically distributed sample  $(Y_i, X_i(\cdot))_{i=1, \dots, n}$ . In order to adapt (4) to functional covariates, we require an estimator of the conditional CDF that uniformly converges to  $F(\cdot|x)$ . For this purpose, we use the Nadaraya-Watson-type estimator suggested by Ferraty et al. (2010), who showed that

$$(8) \quad \hat{F}_{h_F}(y|x) = \frac{\sum_{i=1}^n L_F\left(\frac{\|x - X_i\|}{h_F}\right) 1(Y_i \leq y)}{\sum_{i=1}^n L_F\left(\frac{\|x - X_i\|}{h_F}\right)}.$$

is a uniformly consistent estimator under conditions (A6)–(A10) in appendix A.2.

Now that an appropriate estimator for the conditional CDF is established, we formulate the finite dimensional minimisation problem, i.e.

$$(9) \quad (\hat{\alpha}_\tau, \hat{b}_{\tau,1}, \dots, \hat{b}_{\tau,K}) \\ = \arg \min_{\alpha, b_1, \dots, b_K \in \mathbb{R}} \sum_{i=1}^n J_\tau(\hat{F}_{h_F}(Y_i|x)) \left\{ Y_i - \alpha - \sum_{k=1}^K b_k \langle \phi_k, x - X_i \rangle \right\}^2 L\left(\frac{\|x - X_i\|}{h}\right),$$

where we have used (6) for the finite approximation of the functional coefficient  $\beta(\cdot) \in L^2(\mathcal{S})$ . Notice that (9) is a weighted version of (7) with weights that depend on extremile level  $\tau$ . In particular,  $J_{0.5}(\hat{F}_{h_F}(Y_i|x)) = 1$  for every  $i = 1, \dots, n$ , and so we may recover (7) as a special case corresponding to  $\tau = 0.5$ .

The explicit solutions can also be extended from the ones of extremile regression with scalar data. We define

$$\Phi = \begin{pmatrix} 1 \langle \phi_1, x - X_1 \rangle & \dots & \langle \phi_K, x - X_1 \rangle \\ \vdots & & \vdots \\ 1 \langle \phi_1, x - X_n \rangle & \dots & \langle \phi_K, x - X_n \rangle \end{pmatrix},$$

and hence the solution takes form

$$(10) \quad \begin{pmatrix} \hat{\alpha}_\tau \\ \hat{b}_{\tau,1} \\ \vdots \\ \hat{b}_{\tau,K} \end{pmatrix} = (\Phi^T \mathbf{W}_\tau \Phi)^{-1} \Phi^T \mathbf{W}_\tau \mathbf{Y},$$

where  $\mathbf{Y} = (Y_1, \dots, Y_n)^T$  and  $\mathbf{W}_\tau = \mathbf{W} \mathbf{J}_\tau(F(\mathbf{Y}|x))$ , with  $\mathbf{W} = \text{diag}(L(h^{-1}\|x - X_i\|))_{i=1, \dots, n}$  and  $\mathbf{J}_\tau(F(\mathbf{Y}|x)) = \text{diag}(J_\tau(F(Y_i|x)))_{i=1, \dots, n}$ . From (10) trivially follows that

$$(11) \quad \hat{\alpha}_\tau = \mathbf{e}^T (\Phi^T \mathbf{W}_\tau \Phi)^{-1} \Phi^T \mathbf{W}_\tau \mathbf{Y},$$

and

$$(12) \quad \begin{pmatrix} \hat{b}_{\tau,1} \\ \vdots \\ \hat{b}_{\tau,K} \end{pmatrix} = [\mathbf{0}_K | I_K] (\Phi^T \mathbf{W}_\tau \Phi)^{-1} \Phi^T \mathbf{W}_\tau \mathbf{Y},$$

where  $\mathbf{0}_K = (0, \dots, 0)^T \in \mathbb{R}^K$ ,  $\mathbf{e} = [1, \mathbf{0}_K^T]^T \in \mathbb{R}^{K+1}$  and  $I_K$  is the identity matrix of dimension  $K$ . We denote with  $[\mathbf{0}_K | I_K] \in \mathbb{R}^{K \times K+1}$  the matrix that has  $\mathbf{0}_K$  as first column and coincides with  $I_K$  for the remaining columns. Finally, a natural choice for  $\{\phi_k(\cdot)\}_{k=1}^K$  is the first  $K$  eigenfunctions arising from the spectral decomposition of the estimated covariance operator of the curves  $X_1(\cdot), \dots, X_n(\cdot)$ , as suggested in [Ferraty and Nagy \(2021\)](#).

**3.2. Asymptotic bias.** Let the assumptions (A2)–(A5) of appendix [A.2](#) hold, and from (11), and consider

$$\begin{aligned} \mathbb{E}[\hat{\alpha}_\tau | \mathbf{X}] &= \mathbf{e}^T (\Phi^T \mathbf{W}_\tau \Phi)^{-1} \Phi^T \mathbf{W}_\tau \mathbb{E}[\mathbf{Y} | \mathbf{X}] \\ &= \mathbf{e}^T (\Phi^T \mathbf{W}_\tau \Phi)^{-1} \Phi^T \mathbf{W} \mathbb{E}[\mathbf{J}_\tau(F(\mathbf{Y}|\mathbf{X})) \mathbf{Y} | \mathbf{X}] \\ &= \mathbf{e}^T (\Phi^T \mathbf{W}_\tau \Phi)^{-1} \Phi^T \mathbf{W} (\xi_\tau(X_1), \dots, \xi_\tau(X_n))^T, \end{aligned}$$

where  $\mathbf{X}$  is the sample of functional covariates  $X_1(\cdot), \dots, X_n(\cdot)$ . Denote by  $\mathcal{P}_K^\perp$  the projection onto the orthogonal component of  $\mathcal{F}^K$ , i.e.  $\mathcal{P}_K^\perp f = \sum_{k>K} b_k \phi_k$  for any  $f \in L^2(\mathcal{S})$ ,

where we use the same notation as in (6), with  $b_k = \langle f, \phi_k \rangle$ . Relying on (A1), for any function  $X(\cdot) \in E$  and fixed  $\tau \in (0, 1)$ , the second order Taylor expansion of  $\xi_\tau(X)$  around  $x$  is given a.s. by

$$(13) \quad \xi_\tau(\mathbf{X}) = \xi_\tau(x) + \langle \xi'_{\tau,x}, \mathbf{X} - x \rangle + \frac{1}{2} \langle \xi''_{\tau,\rho}(\mathbf{X} - x), \mathbf{X} - x \rangle$$

$$(14) \quad = \xi_\tau(x) + \langle \mathcal{P}_K \xi'_{\tau,x}, \mathbf{X} - x \rangle + \langle \mathcal{P}_K^\perp \xi'_{\tau,x}, \mathbf{X} - x \rangle + \frac{1}{2} \langle \xi''_{\tau,\rho}(\mathbf{X} - x), \mathbf{X} - x \rangle$$

with  $\rho = x + t(\mathbf{X} - x)$ ,  $t \in (0, 1)$ . Then, plugging in the sample of curves  $X_1(\cdot), \dots, X_n(\cdot)$  in expansion (13), we get

$$(15) \quad \begin{pmatrix} \xi_\tau(X_1) \\ \vdots \\ \xi_\tau(X_n) \end{pmatrix} = \Phi \begin{pmatrix} \xi_\tau(x) \\ \nabla \xi_\tau(x) \end{pmatrix} + \begin{pmatrix} \langle \mathcal{P}_K^\perp \xi'_{\tau,x}, X_1 - x \rangle \\ \vdots \\ \langle \mathcal{P}_K^\perp \xi'_{\tau,x}, X_n - x \rangle \end{pmatrix} + \frac{1}{2} R_{\tau,\rho,x}$$

where  $\nabla \xi_\tau(x) = (\langle \xi'_{\tau,x}, \phi_1 \rangle, \dots, \langle \xi'_{\tau,x}, \phi_n \rangle)^T$ , since  $\langle \mathcal{P}_K^\perp \xi'_{\tau,x}, X_i - x \rangle = \sum_{k=1}^K \langle \xi'_{\tau,x}, \phi_k \rangle \langle \phi_k, X_i - x \rangle$ . Moreover,  $R_{\tau,\rho,x} = (R_{\tau,\rho,x,1}, \dots, R_{\tau,\rho,x,n})^T$ , with  $R_{\tau,\rho,x,i} = \langle \xi''_{\tau,\rho}(X_i - x), X_i - x \rangle$ . Hence, we obtain

$$(16) \quad \mathbb{E}[\hat{\alpha}_\tau | \mathbf{X}] = \xi_\tau(x) + T_1 + \frac{1}{2} T_2$$

with

$$(17) \quad T_1 = \mathbf{e}^T (\Phi^T \mathbf{W}_\tau \Phi)^{-1} \Phi^T \mathbf{W} (\langle \mathcal{P}_K^\perp \xi'_{\tau,x}, X_1 - x \rangle \dots \langle \mathcal{P}_K^\perp \xi'_{\tau,x}, X_n - x \rangle)^T$$

and

$$(18) \quad T_2 = \mathbf{e}^T (\Phi^T \mathbf{W}_\tau \Phi)^{-1} \Phi^T \mathbf{W} R_{\tau,\rho,x}.$$

**THEOREM 3.1** (Asymptotic bias of  $\hat{\alpha}_\tau$ ). *Under conditions (A1) – (A10)*

$$(19) \quad \mathbb{E}[\hat{\alpha}_\tau | \mathbf{X}] = \xi_\tau(x) + \mathcal{O}_{\mathbb{P}}(h \| \mathcal{P}_K^\perp \xi'_{\tau,x} \|) + \frac{1}{2} \mathcal{O}_{\mathbb{P}}(h^2)$$

**3.3. Asymptotic variance.** We now turn to the variance. Using similar arguments to those in Section 3.2, we obtain

$$\begin{aligned} \text{Var}(\hat{\alpha}_\tau | \mathbf{X}) &= [\mathbf{e}^T (\Phi^T \mathbf{W}_\tau \Phi)^{-1} \Phi^T \mathbf{W}_\tau] \text{Var}(\mathbf{Y} | \mathbf{X}) [\mathbf{W}_\tau \Phi (\Phi^T \mathbf{W}_\tau \Phi)^{-1} \mathbf{e}] \\ &= [\mathbf{e}^T (\Phi^T \mathbf{W}_\tau \Phi)^{-1} \Phi^T \mathbf{W}] \text{Var}(\mathbf{J}_\tau(F(\mathbf{Y} | \mathbf{X})) \mathbf{Y} | \mathbf{X}) [\mathbf{W} \Phi (\Phi^T \mathbf{W}_\tau \Phi)^{-1} \mathbf{e}] \end{aligned}$$

By (A5), we may write each entry of diagonal matrix  $\text{Var}(\mathbf{J}_\tau(F(\mathbf{Y} | \mathbf{X})) \mathbf{Y} | \mathbf{X})$  as

$$[\text{Var}(\mathbf{J}_\tau(F(\mathbf{Y} | \mathbf{X})) \mathbf{Y} | \mathbf{X})]_{ii} = \sigma_\tau^2(x) + o(1),$$

for  $i = 1, \dots, n$  and fixed  $\tau \in (0, 1)$ . Hence

$$(20) \quad \text{Var}(\hat{\alpha}_\tau | \mathbf{X}) = [\sigma_\tau^2(x) + o(1)] \mathbf{e}^T (\Phi^T \mathbf{W}_\tau \Phi)^{-1} \Phi^T \mathbf{W}^2 \Phi (\Phi^T \mathbf{W}_\tau \Phi)^{-1} \mathbf{e},$$

where  $\mathbf{W}^2 = \text{diag}((L(h^{-1} \|x - X_i\|))^2)_{i=1, \dots, n}$ .

**THEOREM 3.2** (Asymptotic variance of  $\hat{\alpha}_\tau$ ). *Under conditions (A1) – (A6)*

$$\text{Var}(\hat{\alpha}_\tau | \mathbf{X}) = \mathcal{O}_{\mathbb{P}}(\lambda_K \{n\pi_x(h)\}^{-1}).$$

where  $\lambda_K$  is the smallest eigenvalue of the  $\Gamma$  matrix, defined in appendix A.1.

3.4. *Extremile estimator based on local bandwidth.* In the previous sections we have considered a global bandwidth  $h$  that goes to zero as the sample size increases as dictated by (A3). We now consider two options for a data-driven local bandwidth selection for finite samples.

The first one we consider is inspired by the bandwidth selected via  $k$ -nearest neighbours (kNN) algorithm suggested by [Ferraty and Nagy \(2021\)](#) for mean scalar-on-function local linear regression. More specifically, consider a finite collection of bandwidths  $H$ . For every  $i = 1, \dots, n$ , the local bandwidth is

$$(21) \quad h_i^k = \inf \left\{ h \in H : \sum_{j=1, j \neq i}^n \mathbf{1}_{X_j \in B_h(x)} = k \right\},$$

namely the minimal radius of the ball centered in  $x$  that contains exactly  $k$  functional independent variables not including  $X_i(\cdot)$ . Then the extremile estimator based on the kNN local bandwidth is

$$(22) \quad \hat{\alpha}_\tau^\ell = \mathbf{e}^T (\Phi^T \mathbf{W}_\tau^\ell \Phi)^{-1} \Phi^T \mathbf{W}_\tau^\ell \mathbf{Y},$$

where  $\mathbf{Y} = (Y_1, \dots, Y_n)^T$  and  $\mathbf{W}_\tau^\ell = \mathbf{W}^\ell \mathbf{J}_\tau(F(\mathbf{Y}|x))$ , and where we now have  $\mathbf{W}^\ell = \text{diag} \left( L((h_i^k)^{-1} \|x - X_i\|) \right)_{i=1, \dots, n}$  and  $\mathbf{J}_\tau(F(\mathbf{Y}|x)) = \text{diag} (J_\tau(F(Y_i|x)))_{i=1, \dots, n}$ . The following theorem shows the asymptotic behaviour of estimator (22).

**THEOREM 3.3.** *(Asymptotic behaviour of  $\hat{\alpha}_\tau^\ell$ ) Under (A1)-(A3) and (A5)-(A7), we have*

$$(23) \quad \hat{\alpha}_\tau^\ell(x) - \xi_\tau(x) = \mathcal{O}_{\mathbb{P}} \left( \|\mathcal{P}_K^\perp \zeta'_{\tau,x}\| \pi_x^{-1} \left( \frac{k}{n} \right) \right) + \mathcal{O}_{\mathbb{P}} \left( \left( \pi_x^{-1} \left( \frac{k}{n} \right) \right)^2 \right) + \mathcal{O}_{\mathbb{P}}(k^{-1/2}).$$

The second option takes bandwidth (21) as a building block for an extremile level-dependent bandwidth. Using the same idea as in the supplementary materials of [Daouia, Gijbels and Stupfler \(2022\)](#), for a fixed  $\tau \in (0, 1)$ , the adaptive local bandwidth is given by

$$(24) \quad h_{\tau,i}^k = h_i^k \left[ V_{K_\tau \circ \Phi} \cdot (J_\tau(\tau) \cdot \phi(\Phi^{-1}(\tau)))^2 \frac{4\tau(1-\tau)}{(\phi(\Phi^{-1}(\tau)))^2} \right]^{1/5}$$

$$(25) \quad = h_i^k \left[ 4\tau(1-\tau) V_{K_\tau \circ \Phi} (J_\tau(\tau))^2 \right]^{1/5}$$

$$(26) \quad = h_i^k \left[ 4\tau(1-\tau) \left( \int_0^1 (\Phi^{-1}(t) - \mu_\tau)^2 J_\tau(t) dt \right) (J_\tau(\tau))^2 \right]^{1/5}$$

where  $\Phi^{-1}(\cdot)$  and  $\mu_\tau = \int_0^1 \Phi^{-1}(t) J_\tau(t) dt$  are the quantile function and the true extremile of level  $\tau$  of a standard Gaussian distribution, respectively.

3.5. *Bandwidth selection for conditional CDF estimator.* In order to pick a data-driven bandwidth for estimator (8) we rely on the work of [Chagny and Roche \(2014\)](#), which is based on a trade-off between bias and variance. We briefly overview such selection method in this section.

Consider data  $\{Y_i, X_i(\cdot)\}_{i=1}^n$  and bandwidth  $h_F \in H_F$ , where  $H_F$  is a finite set of positive bandwidths with cardinality depending on the sample size  $n$ . Then, the small ball probability of function  $X \in E$ , drawn from the distribution of random variable  $X(\cdot)$ , of being in a neighborhood centered in  $x(\cdot) \in E$  of radius  $h_F$ , namely

$$\pi_x(h_F) = \mathbb{P}(\|X - x\| \leq h_F),$$

is approximated by

$$\hat{\pi}_x(h_F) = \frac{1}{n} \sum_{i=1}^n \mathbf{1}_{\{|X_i - x| \leq h_F\}},$$

assuming that the data in the sample are iid realisations from the same distribution of  $X(\cdot)$ . Moreover, let  $\mathcal{I}_Y \subset \mathbb{R}$  the interval in which  $Y_1, \dots, Y_n$  lie and  $\|\hat{F}_{h_F}(x)\| = \int_{\mathcal{I}_Y} \hat{F}_{h_F}(y|x) dy$ . Then, bandwidth  $h_F^{\text{opt}}$  for estimator  $\hat{F}_{h_F}(\cdot|x)$  is chosen such that it minimizes a trade-off between an approximation of the bias and an upper bound of the variance of such estimator. Concretely, define

$$(27) \quad \hat{V}(h_F, x) = \begin{cases} \kappa \frac{\ln n}{n \ln \hat{\pi}_x(h_F)} & \text{if } \hat{\pi}_x(h_F) \neq 0, \\ +\infty & \text{otherwise,} \end{cases}$$

and

$$(28) \quad \hat{A}(h_F, x) = \max_{h'_F \in H_F} \left( \|\hat{F}_{h'_F}(x) - \hat{F}_{h_F \vee h'_F}(x)\|_{\mathcal{I}_Y} - \hat{V}(h'_F, x) \right)_+.$$

Then

$$(29) \quad h_F^{\text{opt}}(x) = \arg \min_{h_F \in H_F} \left( \hat{A}(h_F, x) + \hat{V}(h_F, x) \right),$$

where  $\kappa > 0$ .  $\hat{A}(h)$  and  $\hat{V}(h)$  are the approximations of bias term and upper bound of variance term, respectively.

In order to compute the optimal bandwidth for the  $i$ -th covariate  $X_i(\cdot)$ , i.e.  $h_F^{\text{opt}}(X_i)$  for  $i = 1, \dots, n$ , we use a leave-one-out procedure, taking  $Y_1, \dots, Y_{i-1}, Y_{i+1}, \dots, Y_n$  and  $X_1(\cdot), \dots, X_{i-1}(\cdot), X_{i+1}(\cdot), \dots, X_n(\cdot)$  as sample, and centering (27), (28) and (29) in  $X_i(\cdot)$ . Notice that, as explained in (Chagny and Roche, 2014, Section 6), the choice of  $\kappa$  controls the bias-variance trade-off, and small values of the parameter lead to smaller values of  $\{h_F^{\text{opt}}(X_i)\}_i$ .

**4. Simulations.** In this section we present a simulation study which highlight relevant features of the proposed methodology. We generate functions on a regular dense grid  $\mathcal{S} = [0, 1]$ . Specifically, we have that

$$X_i(s) = c_{0i} + c_{1i}\psi_1(s) + c_{2i}\psi_2(s) + c_{3i}\psi_3(s) + c_{4i}\psi_4(s), \quad i = 1, \dots, n, s \in \mathcal{S},$$

with  $\psi_1(s) = \sin(\pi s)$ ,  $\psi_2(s) = \cos(10\pi s)$ ,  $\psi_3(s) = \sin(30\pi s)$  and  $\psi_4(s) = \cos(40\pi s)$ , and coefficients  $c_{0i} \stackrel{iid}{\sim} \mathcal{N}(2, 1)$ ,  $c_{1i} \stackrel{iid}{\sim} \mathcal{N}(2, 0.25)$ ,  $c_{2i} \stackrel{iid}{\sim} \mathcal{N}(0, 0.25)$ ,  $c_{3i} \stackrel{iid}{\sim} \mathcal{N}(0, 0.05)$  and  $c_{4i} \stackrel{iid}{\sim} \mathcal{N}(0, 0.05)$ . In the first panel of Figure 1 we show a realisation of  $\{X_i(\cdot)\}_i$ , with three random curves highlighted. Our aim is to simulate data that is similar to temperature and wind speed profiles in our application, including more local variation to test the robustness of our methodology.

We construct a scalar-on-function regression model as follows:

$$(30) \quad Y_i = \beta_0 + \int_{\mathcal{S}} \beta(s) X_i(s) ds + \sigma(X_i) \epsilon_i, \quad i = 1, \dots, n,$$

with  $\epsilon_i \stackrel{iid}{\sim} \mathcal{N}(0, \sigma_\epsilon^2)$  independent of  $\{X_i(\cdot)\}_{i=1}^n$ , and where  $\sigma(X_i)$  controls the heteroskedasticity of the model. In our simulation study,  $\sigma_\epsilon^2 = 0.25$ . In order to compute the true conditional extremile of level  $\tau$  corresponding to the model, we may use (Daouia, Gijbels and

Stupfler, 2022, Proposition 2), where a relationship between extremiles and quantiles is provided. Given level  $\tau \in (0, 1)$  the conditional extremile  $\xi_\tau(x)$  defined in (1) can be computed through conditional quantile  $q_t(x)$  as follows

$$(31) \quad \xi_\tau(x) = \int_0^1 q_t(x) dK_\tau(t).$$

Then  $\mathbb{P}(Y_i \leq q_t(X_i)) = t$  and

$$\begin{aligned} \mathbb{P}\left(\frac{\epsilon_i}{\sigma_\epsilon} \leq \frac{q_t(X_i) - \beta_0 - \int_{\mathcal{S}} \beta(s) X_i(s) ds}{\sigma_\epsilon \sigma(X_i)}\right) &= t, \\ \frac{q_t(X_i) - \beta_0 - \int_{\mathcal{S}} \beta(s) X_i(s) ds}{\sigma_\epsilon \sigma(X_i)} &= \Phi^{-1}(t), \end{aligned}$$

where  $\Phi(\cdot)$  is the CDF of a standard Gaussian random variable. Hence, the conditional quantile of model (30) is

$$q_t(X_i) = \beta_0 + \int_{\mathcal{S}} \beta(s) X_i(s) ds + \sigma_\epsilon \sigma(X_i) \Phi^{-1}(t),$$

and consequently the conditional extremile of level  $\tau$  is

$$\begin{aligned} \xi_\tau(X_i) &= \int_0^1 q_t(X_i) dK_\tau(t) \\ &= \int_0^1 q_t(X_i) J_\tau(t) dt \\ &= \left( \beta_0 + \int_{\mathcal{S}} \beta(s) X_i(s) ds \right) \int_0^1 J_\tau(t) dt + \sigma_\epsilon \sigma(X_i) \int_0^1 \Phi^{-1}(t) J_\tau(t) dt \\ (32) \quad &= \beta_0 + \int_{\mathcal{S}} \beta(s) X_i(s) ds + \sigma_\epsilon \sigma(X_i) \xi_{\epsilon, \tau}, \end{aligned}$$

where, using (31),  $\xi_{\epsilon, \tau}$  is the extremile of order  $\tau$  of a standard Gaussian distribution. Notice that the last equality holds since  $\int_0^1 J_\tau(t) dt = 1$ .

In our simulation study we choose intercept  $\beta_0 = 0$  and functional coefficient  $\beta(s) = 2 \cos(2\pi s)$ , with  $s \in \mathcal{S} = [0, 1]$ . Moreover, we pick

$$(33) \quad \sigma(X_i) = 1 + \gamma \int_{\mathcal{S}} X_i(s) ds,$$

with  $\gamma \geq 0$ . In particular, we consider two types of model, namely the *homoskedastic* model with  $\gamma = 0$ , and the *heteroskedastic* model where  $\gamma > 0$ . Notice that having a homoskedastic model entails that conditional extremes of different levels differ only by a shift of  $\sigma_\epsilon \xi_{\epsilon, \tau}$ , while in heteroskedastic models the variance of the extremile is influenced by the covariates depending on the magnitude of  $\gamma$ . To illustrate this behaviour, we show the extremiles at three levels when  $\gamma = 0$  and  $\gamma = 1$  in the second and third panels of Figure 1, respectively. We consider  $\gamma = \{0, 0.5, 1, 2\}$ , and for each heteroskedasticity level we simulate  $B = 500$  samples with  $n = 200$  observations and with  $\mathcal{S}$  is discretized with a regular grid of 100 points. At each repetition, we estimate conditional extremiles of levels  $\tau = \{0.1, 0.2, 0.3, 0.5, 0.7, 0.8, 0.9\}$ .

In order to measure the estimation accuracy, we compute the Mean Squared Error (MSE) for every iteration  $b = 1, \dots, B$ , more specifically for each value of  $\gamma$  and each level  $\tau$  we compute

$$(34) \quad \text{MSE}_b(\tau, \gamma) = \frac{1}{n} \sum_{i=1}^n (\xi_{\tau, b}^\gamma(X_i) - \widehat{\xi}_{\tau, b}^\gamma(X_i))^2,$$

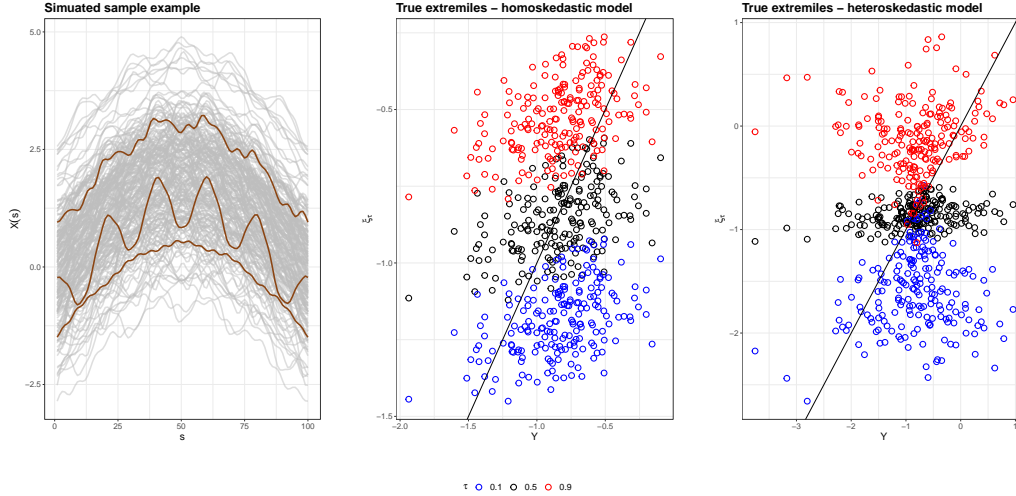


FIG 1. The first panel shows an example of simulated functional sample, with three random curves highlighted. The remaining panels show true extremiles plotted against responses in case  $\gamma = 0$  (second panel) and  $\gamma = 1$  (third panel). The extremiles and responses correspond to functional model (32) when the covariates are those shown in the first panel.

where we denote with  $\xi_{\tau,b}^{\gamma}(X_i)$  the true extremile of level  $\tau$  generated with value  $\gamma$  in (33) for the  $b$ -th dataset, and with  $\hat{\xi}_{\tau,b}^{\gamma}(X_i)$  its estimated counterpart. All extremiles were computed with  $\kappa = 1$  in (27). In each panel of Figure 2 we show the boxplots of MSE on the log-scale for the four simulation settings, positioned in increasing level of heteroskedasticity from left to right. The boxplots relative to MSE at different extremile levels are colored from blue to red from the lowest to the highest. The homoskedastic case, i.e. when  $\gamma = 0$ , is the one with lower MSE overall. In particular, we notice that the error symmetrically increases as  $\tau$  is lower and higher than 0.5, to which corresponds the MSE with larger variability. This is also true for  $\gamma = 0.5$ , but the MSE for  $\tau = 0.3, 0.5, 0.7$  seems comparable. The scenarios corresponding to  $\gamma = 1$  and  $\gamma = 2$  have comparable MSE across extremile levels, and the error at  $\tau = 0.2, 0.3, 0.5, 0.7, 0.8$  is centered around the same value. Finally, across all scenarios, the most extreme levels, namely  $\tau = 0.1$  and  $\tau = 0.9$ , are those with higher MSE. This is not surprising, as  $J_{\tau}(\cdot)$  exponentially decreases close to 0 and exponentially increases close to 1 for the two levels, respectively.

**5. Application to Swiss climate scenarios.** In this section we analyze data which is part of the CH2018 Swiss Climate Change Scenarios project<sup>1</sup> (CH2018, 2018; Sørland et al., 2020; Fischer et al., 2022). Such study investigates the impact of climate change in Switzerland in scenarios where different degrees of actions for climate mitigation are applied. Our goal is to quantify the effect of such measures by means of the statistical tools studied in Section 3. In particular, we are interested in verifying whether future summers will be hotter and drier if no preventive measures were applied starting from the present day.

<sup>1</sup><https://www.nccs.admin.ch/nccs/en/home/climate-change-and-impacts/swiss-climate-change-scenarios.html>

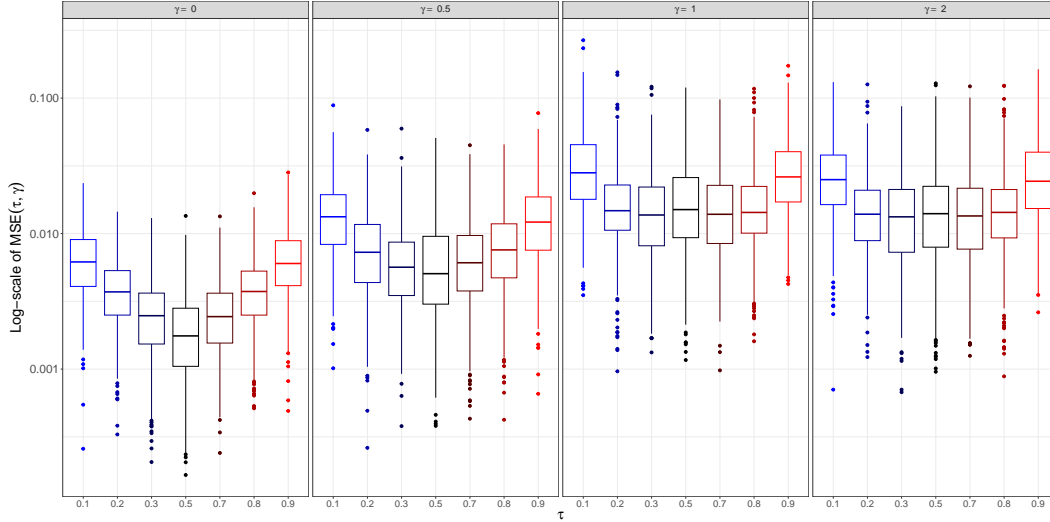


FIG 2. MSE values as in (34) on the log-scale for four different simulation studies characterized by different values of  $\gamma$  (from left to right panel by increasing magnitude). For each of them, we show the boxplots for different extremile levels, namely  $\tau = 0.1, 0.2, 0.3, 0.5, 0.7, 0.8, 0.9$ .

5.1. *Data description.* The datasets (CH2018 Project Team, 2018), available online<sup>2</sup>, consist of simulations of several weather variables for  $n = 41$  weather stations in Switzerland for each month of the year. Among the climatic variables simulated hourly are air temperature at 2 meters above the ground, wind speed and relative humidity. We consider two scenarios representative of the climatic situation of Switzerland in the mid century, i.e. in the period between 2045 and 2074: one where efforts against climate change have been made since the present day, called RCP2.6, and one where no measures have been applied, called RCP8.5. Moreover, the information is provided for both a Design Reference Year (DRY) or a year with an exceptionally Warm Summer (WS). Within the same scenarios, the measurements of DRY and WS years only differ from mid April to mid October. Hence, we analyse the months between May and September. We consider the smoothed monthly averaged air temperatures,  $\{\overline{Temp}_{im}(\cdot)\}_{im}$ , and the monthly averaged wind speed  $\{\overline{Wind}_{im}(\cdot)\}_{im}$ , with  $m = 5, \dots, 9$  indicating the month. Such curves were obtained by smoothing the pointwise average over the days  $d = 1, \dots, D_m$  in each month  $m$  for each station  $i$ , i.e.

$$\frac{1}{D_m} \sum_{d=1}^{D_m} Temp_{imd}(h), \quad i = 1, \dots, n, m = 5, \dots, 9, h = 1, \dots, 24$$

$$\frac{1}{D_m} \sum_{d=1}^{D_m} Wind_{imd}(h), \quad i = 1, \dots, n, m = 5, \dots, 9, h = 1, \dots, 24$$

over a dense regular grid  $S$  representing the hours of the day.

In Figure 3 we see that temperatures are generally higher, reaching their peak in the early afternoon, in the RCP8.5 scenario than in the RCP2.6 one, showing how not implementing actions against climate change will lead to generally warmer summers. This holds true in both DRY and WS cases. As the CH2018 Swiss Climate Change Scenarios project is focussed on studying the impact of climate change in cities, we highlight the temperature profiles of

<sup>2</sup><https://www.meteoswiss.admin.ch/climate/climate-change/swiss-climate-change-scenarios/climate-scenarios-indoor-climate.html>

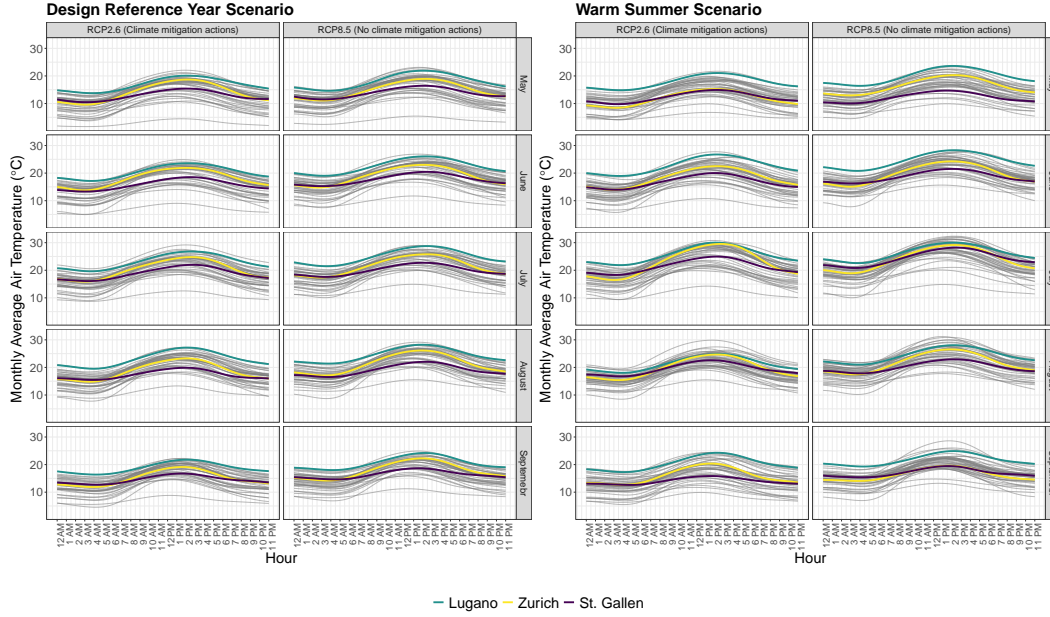


FIG 3. Monthly averages of air temperature profiles for the 41 weather stations, divided by DRY (first panel) and WS (second panel) cases. For each case, we consider the RCP2.6 and RCP8.5 scenarios (first and second columns, respectively). We show the months from May to September, from the first to the last row. All curves are in grey, with the exception to those referring to Lugano (in green), Zurich (in yellow), and St. Gallen (in aubergine).

three Swiss cities with rather different geographical locations, namely Lugano, Zurich and St.Gallen. Specifically, Lugano is located by a lake, and its temperature is one of the highest in the sample, while Zurich's location is a plain, and its temperature varies more between day to night hours than the one of St. Gallen, which is located on a slope. Figure 4 shows the monthly averaged wind speeds, and it seems like there is not a striking difference between the scenarios. We notice that the three cities we are interested in have lower peaks than other stations. This is not surprising, as urban environments are less exposed to winds due to the shielding provided by buildings. However, we see that the wind speed in St. Gallen is more stable than for the other two cities.

5.2. *Estimated extremiles for Swiss cities.* We now analyse the estimated conditional extremiles of different levels. We fit model (9) separately for each month  $m = 5, \dots, 9$  in two different settings: One where we take the monthly average of hourly relative humidity as response and the monthly average temperature shown in Figure 3, and the other where we take the monthly average of hourly air temperature as response and the monthly average wind speed shown in Figure 4. Specifically, the responses considered are

$$\overline{\overline{Hum}}_{im} = \frac{1}{24} \sum_{h=1}^{24} \left[ \sum_{d=1}^{D_m} Hum_{imd}(h) \right] \quad i = 1, \dots, n, m = 5, \dots, 9,$$

$$\overline{\overline{Temp}}_{im} = \frac{1}{24} \sum_{h=1}^{24} \left[ \sum_{d=1}^{D_m} Temp_{imd}(h) \right] \quad i = 1, \dots, n, m = 5, \dots, 9.$$

We fit models for scenarios RCP2.6 and RCP8.5 separately, as we do for the reference year and warm summer cases, though we avoid making this explicit in the notation. Moreover,

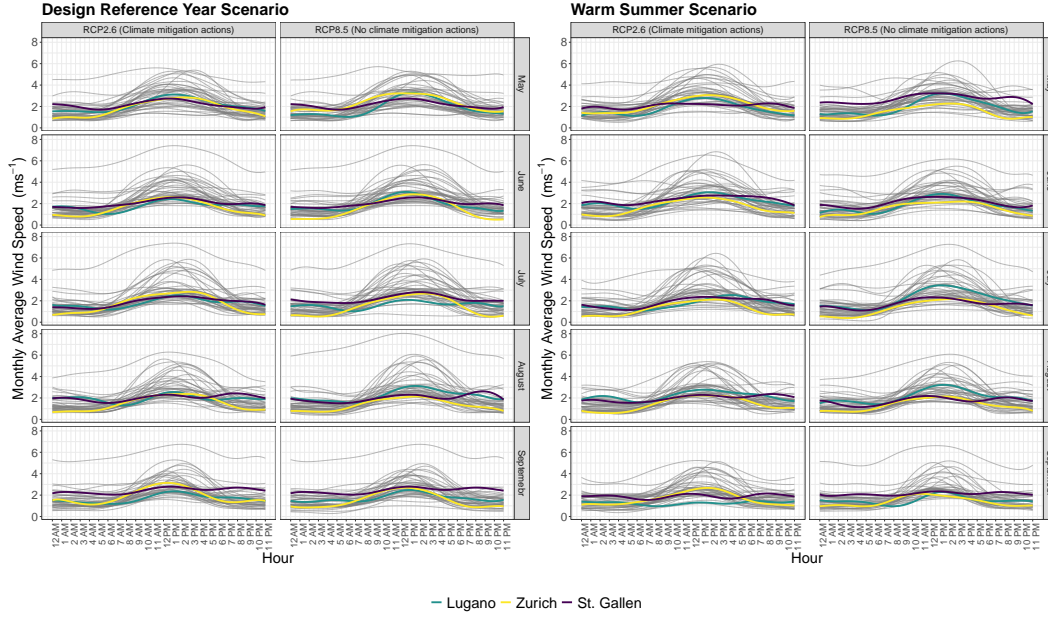


FIG 4. Monthly averages of wind speed profiles for the 41 weather stations, divided by DRY (first panel) and WS (second panel) cases. For each case, we consider the RCP2.6 and RCP8.5 scenarios (first and second columns, respectively). We show the months from May to September, from the first to the last row. All curves are in grey, with the exception to those referring to Lugano (in green), Zurich (in yellow), and St. Gallen (in aubergine).

we use  $\kappa = 4$  and  $|H_F| = 20$  in the procedure for the bandwidth selection of the conditional CDF estimator described in Section 3.5.

In Figure 5 the estimated conditional extremiles of sample  $\left\{ \overline{Hum}_{im}, \overline{Temp}_{im}(\cdot) \right\}_{im}$  for each month are shown. In particular, we focus on levels  $\tau = 0.5$ , corresponding to the local linear mean estimator, and  $\tau = 0.1$ . First, we notice that extremiles at both levels seem generally higher in the reference year case compared to the warm summer case, which is characterized by a larger difference between extremiles in RCP2.6 and RCP8.5 overall. The relative humidity levels are particularly critical in June and July. The lowest estimated extremiles at level 0.1 in the reference year case are and in the RCP2.6 scenario are 62.2% and 58.04% for the two months respectively, while their counterparts in the RCP8.5 scenario are 52.74% and 55.6%. In the warm case scenario, the minima of  $\xi_{0.1}$  in the two months are 54.58% and 53.25% in the RCP2.6 scenario, while in the RCP8.5 scenario are 45.84% and 45.53%. As far as the three cities are concerned, Table 1 shows the estimated extremiles in the month of July in detail. Firstly we notice that the absolute difference of the corresponding extremiles at same level but different climate scenarios are larger in the warm summer case than in the reference year case. Moreover, the extremiles corresponding to RCP2.6 are not always higher than those of RCP8.5. For instance, Zurich is more humid in the RCP8.5 scenario in both cases at  $\tau = 0.5$  and in the warm summer case at  $\tau = 0.1$ . This holds true for St. Gallen in the reference year case and level 0.1 as well. In the reference year case, Lugano is always dryer, even though the difference between its corresponding estimated extremiles with that of the other two cities for  $\tau = 0.5$  is much larger than for  $\tau = 0.1$ . Lugano is the driest city in the warm summer case as well, with the exception of scenario RCP2.6 at level 0.1, where Zurich has a slightly lower extremile.

Figure 6 shows the estimated conditional extremiles of data  $\left\{ \overline{Temp}_{im}, \overline{Wind}_{im}(\cdot) \right\}_{im}$ . In general, the estimated extremiles are higher in the scenario where no climate actions were

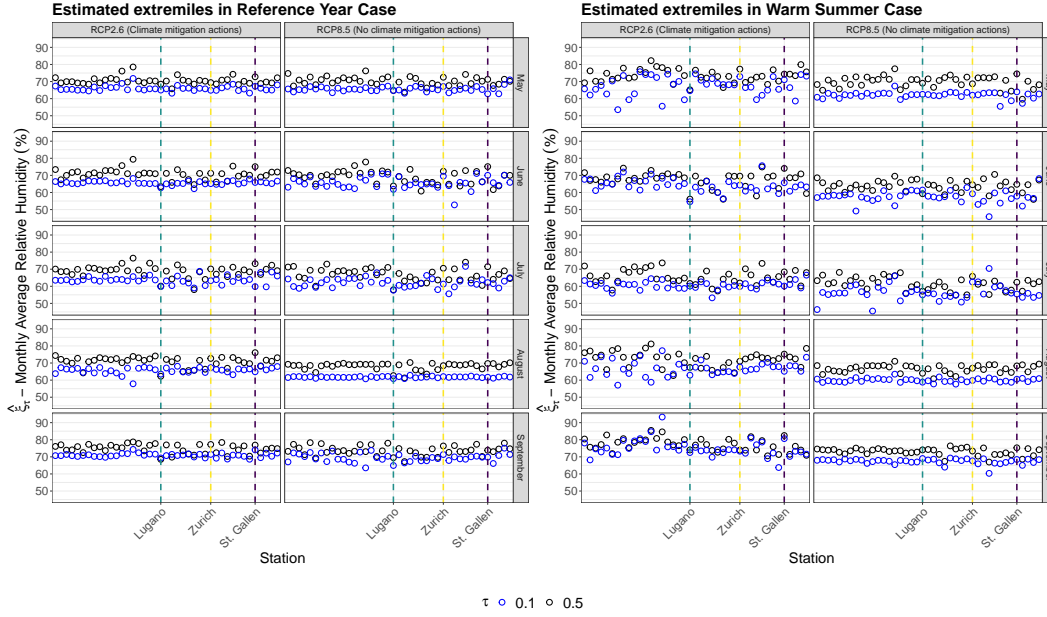


FIG 5. Estimated extremiles of relative humidity conditional on temperature at levels  $\tau = 0.5$  (in black) and  $\tau = 0.1$  (in blue) for all the weather stations for the months between May and September. The DRY and WS cases are shown in the first and second panel, respectively. Moreover, we show the results for scenario RCP2.6 in the first columns, and those for scenario RCP8.5 in the second.

applied for all months considered. For instance, in the months of June and July and in the reference year case the maxima of  $\hat{\xi}_{0.9}$  are 20.18°C and 23.59°C in RCP2.6 scenario, and 22.53°C and 24.11°C in RCP8.5 scenario, respectively. On the other hand, the estimated extremiles in the warm summer case increase: during the same months, the maxima are 22.39°C and 25.55°C, and 25.02°C and 28.5°C in the RCP2.6 and RCP8.5 scenarios, respectively. Such trend is also true for the estimated extremiles of the three cities in the month of July shown in Table 2, with the exception of  $\hat{\xi}_{0.5}$  of Lugano in the warm summer case, where the temperature is slightly higher in the scenario where no preventive measures against climate change were put into action. In particular, we notice that the temperatures of the three cities are very similar in the reference year case and RCP2.6 scenario for both extremile levels. This is also true for  $\tau = 0.5$  in the same case, but there is larger variation among the cities for the local linear mean estimator. Interestingly, in the warm summer case the warmest city (at both extremile levels) differs depending on the climate scenario: it is Lugano in RCP2.6 and it is Zurich in RCP8.5.

5.3. *Predicted extremiles in the month of July.* In this section we study the predicted extremiles of the two models presented in Section 5.2. For each case (DRY and WS) and each climate scenario (RCP2.6 and RCP8.5), we consider shifts of the mean functions over the weather station recordings in the month of July, namely

$$(35) \quad AvgTemp_7(s) = \frac{1}{n} \sum_{i=1}^n \overline{Temp}_{i7}(s), \quad s \in \mathcal{S},$$

$$(36) \quad AvgWind_7(s) = \frac{1}{n} \sum_{i=1}^n \overline{Wind}_{i7}(s), \quad s \in \mathcal{S}.$$

TABLE 1

Estimated extremiles  $\hat{\xi}_\tau$  at levels  $\tau = 0.5, 0.1$  of relative humidity for three Swiss cities in the month of July.

		Reference Year Case		Warm Summer Case	
Station		RCP2.6	RCP8.5	RCP2.6	RCP8.5
$\tau = 0.5$	Lugano	60.11%	57.96%	61.64%	57.14%
	Zurich	70.13%	70.54%	61.92%	65.84%
	St. Gallen	73.25%	71.50%	68.42%	62.36%
$\tau = 0.1$	Lugano	59.81%	57.71%	60.17%	54.97%
	Zurich	63.29%	61.31%	59.89%	62.53%
	St. Gallen	59.82%	62.18%	60.12%	55.46%

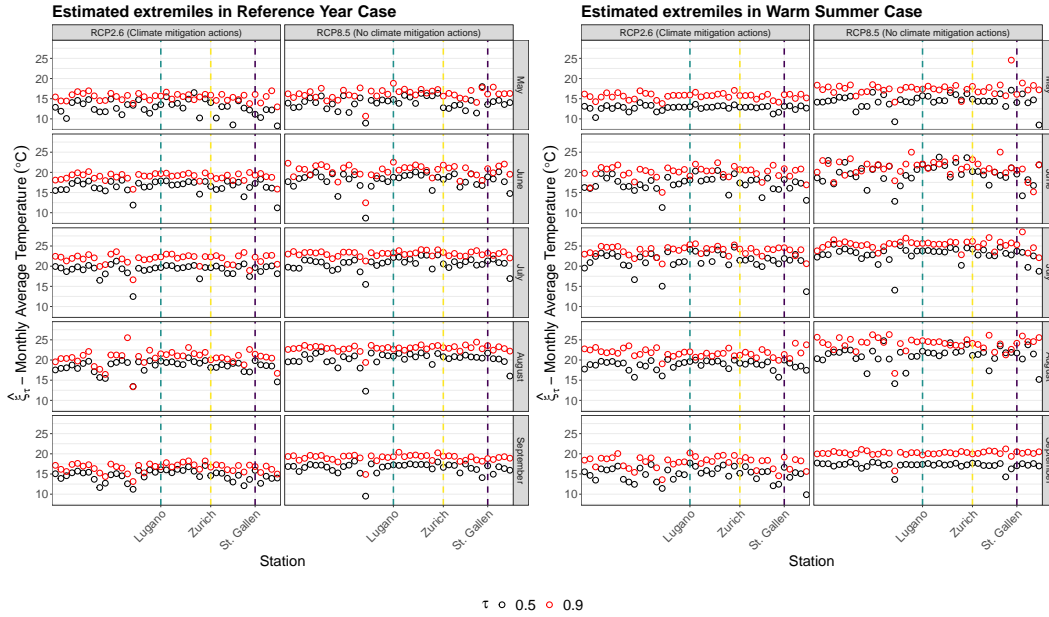


FIG 6. Estimated extremiles of temperature conditional on wind speed at levels  $\tau = 0.5$  (in black) and  $\tau = 0.9$  (in red) for all the weather stations for the months between May and September. The DRY and WS cases are shown in the first and second panel, respectively. Moreover, we show the results for scenario RCP2.6 in the first columns, and those for scenario RCP8.5 in the second.

The covariates we use to predict the conditional extremiles are  $\left\{ AvgTemp_\tau(\cdot) + \Delta_j^{(Temp)} \right\}_j$  and  $\left\{ AvgWind_\tau(\cdot) + \Delta_j^{(Wind)} \right\}_j$ , where  $\Delta^{(Temp)} = \left( \Delta_1^{(Temp)}, \dots, \Delta_{31}^{(Temp)} \right)$   $= [-1.5, \dots, 0, \dots, 1.5]$  and  $\Delta^{(Wind)} = \left( \Delta_1^{(Wind)}, \dots, \Delta_{31}^{(Wind)} \right) = [-0.75, \dots, 0, \dots, 0.75]$ . Thus, we predict the extremile conditional of the two means (35) and (36), and shifts of them, shown in Figures 11 and 12 in the appendix. Notice that we study the four frameworks separately: the mean functions over the weather station are different (we omit additional notation in (35) and (36) for readability), but we apply to them the same shifts  $\Delta^{(Temp)}$  and  $\Delta^{(Wind)}$ . For the local bandwidth selection of the conditional CDF estimation, the predictions are carried out with  $\kappa = 1$  and  $|H_F| = 20$ .

In Figure 7 we show the predicted conditional extremiles of relative humidity against  $\Delta^{(Temp)}$ . First of all, we notice that the the relative humidity is generally higher in the reference year case compared to the warm summer case. In the former, when climate mit-

TABLE 2

Estimated extremiles of air temperature for three Swiss cities in the month of July at levels  $\tau = 0.5$  and  $\tau = 0.9$ .

		Reference Year Case		Warm Summer Case	
		RCP2.6	RCP8.5	RCP2.6	RCP8.5
$\tau = 0.5$	Lugano	19.67°C	22.15°C	24.16°C	23.80°C
	Zurich	19.65°C	20.57°C	21.44°C	24.23°C
	St. Gallen	19.66°C	21.30°C	21.90°C	23.74°C
$\tau = 0.9$	Lugano	22.29°C	23.29°C	25.36°C	25.66°C
	Zurich	22.29°C	23.42°C	24.24°C	26.16°C
	St. Gallen	22.24°C	23.22°C	24.57°C	25.33°C

igation actions were put into place, the relative humidity level slowly decreases as temperature increases for all extremile levels. This is not the case for the scenario where no preventive measures against climate change were taken, where all predicted extremiles seem to be constant around  $\Delta^{(Temp)} = 0$ , i.e. close to  $AvgTemp_{\tau}(\cdot)$ , and decrease in  $\Delta^{(Temp)} \in [-1.5, -0.5] \cup [0.5, 1.5]$ . In the warm summer case, the predicted extremiles corresponding to the RCP2.6 scenario are overall constant, even though those of levels 0.1 and 0.5 seem slightly cyclical. On the other hand, all predicted extremiles corresponding to the RCP8.5 scenario are increasing until and then plateauing around  $\Delta^{(Temp)} = 1$ . Thus, from Figure 7 we may draw two conclusions. First, the “worst case scenario”, namely the predicted extremile of level  $\tau = 0.1$ , is significantly lower in the RCP8.5 scenarios, reaching minima of 59.28% in the reference year case, compared to the RCP2.6 counterpart of 63.13%, and 57.32% in the warm summer case, where the minimum in the RCP2.6 scenario is 58.33%. Secondly, the behaviour of predicted extremiles is not only different between the scenario where actions against global warming were taken compared to the one where they were not, but also between reference year and warm summer scenarios.

Figure 8 shows the predicted extremiles of air temperature for different values of  $\Delta^{(Wind)}$ . In the reference year case and when climate mitigation actions are applied,  $\hat{\xi}_{\tau}$  are decreasing for every level. In the same case but in the RCP8.5 scenario, the predicted extremiles at levels 0.5 and 0.9 are still decreasing but with a smaller slope with respect to their RCP2.6 counterparts, while at levels 0.7 and 0.8 they are overall constant. Moreover, not surprisingly the predicted extremiles of temperature are higher when no climate mitigation actions were taken compared to when they were implemented. We notice a similar behaviour in the warm summer scenario case: In the RCP2.6 scenario, the predicted extremiles are decreasing, while in the RCP8.5 one, they are constant over shifts (with the exception of  $\hat{\xi}_{0.5}$  when  $\Delta^{(Wind)} \in [0.4, 0.75]$ ). Thus, we see that, in case climate mitigation actions are not in place, temperatures will be in general higher, where  $\hat{\xi}_{0.9}$  reaches 23.45°C in a reference year and 25.36°C in the warm summer case, regardless of the wind speed.

**6. Discussion.** In this work we adapted the scalar-on-function local-linear mean regression introduced by [Ferraty and Nagy \(2021\)](#) to extremile scalar-on-function regression. To do so, inspired by [Daouia, Gijbels and Stupfler \(2022\)](#), we chose weights that are functions of the conditional CDF. We made the estimation as automatized as possible by performing kernel estimation twice. First, we estimate the conditional CDF with the Nadaraya-Watson estimator adapted to functional covariates ([Ferraty et al., 2010](#)). For the choice of local bandwidth we use data-driven method introduced by [Chagny and Roche \(2014\)](#). Second, we adapt the local bandwidth choice of [Ferraty and Nagy \(2021\)](#) by rescaling as [Daouia, Gijbels and Stupfler \(2022\)](#) suggests, so as to make it extremile level-dependent. Notice that the choice of bandwidth in both cases is extremely important: in the former, it controls the extremile

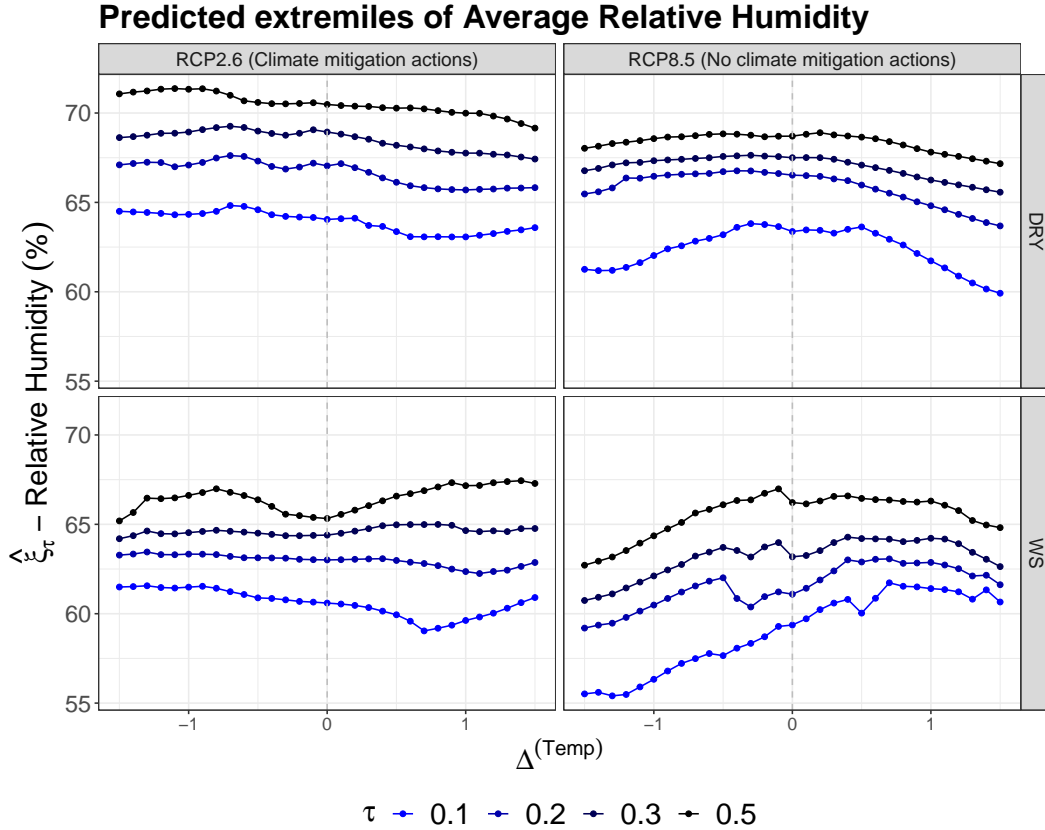


FIG 7. Predicted extremiles at levels  $\tau = 0.1, 0.2, 0.3, 0.5$  (in shades from blue to black) of relative humidity for shifts of the average air temperature of the month of July. For both reference year (first row) and warm summer (second row) cases, we show both RCP2.6 and RCP8.5 scenarios, in the first and second columns, respectively.

crossing, while in the latter it controls the “influence” the sample has on the estimated extremile.

Thus, we studied the asymptotic bias and variance of the resulting estimator, proving rates of asymptotic unbiasedness and consistency, and we tested the developed methodology with a simulation study. All the proposed methods are implemented in R (R Core Team, 2023) with package `ExtrFunReg` (Battagliola, 2024), found at <https://github.com/LauraBattagliola/ExtrFunReg>, and based on version 0.0.2 of package `fl1r`<sup>3</sup>, which is the implementation of the methodology introduced by Ferraty and Nagy (2021).

Finally, we applied the proposed methodology to study the impact of climate change mitigation actions in Switzerland. More specifically, we aimed at understanding whether summers in the future will get warmer and dryer based on simulated datasets provided as part of the CH2018 Swiss Climate Change Scenarios project. From our findings, we obtain, among other things, that that is indeed a generally accurate conclusion. We showed that certain Swiss cities will be warmer from May to September and dryer in the months of June and July in case no climate actions were put into place, both in the case of a reference year and in one of a particularly warm summer. Moreover, with our further analysis we uncovered that the behaviour of climatological phenomena differ depending on whether actions against climate change are in place or not, indicating

<sup>3</sup><https://bitbucket.org/StanislavNagy/fl1r/src/master/>

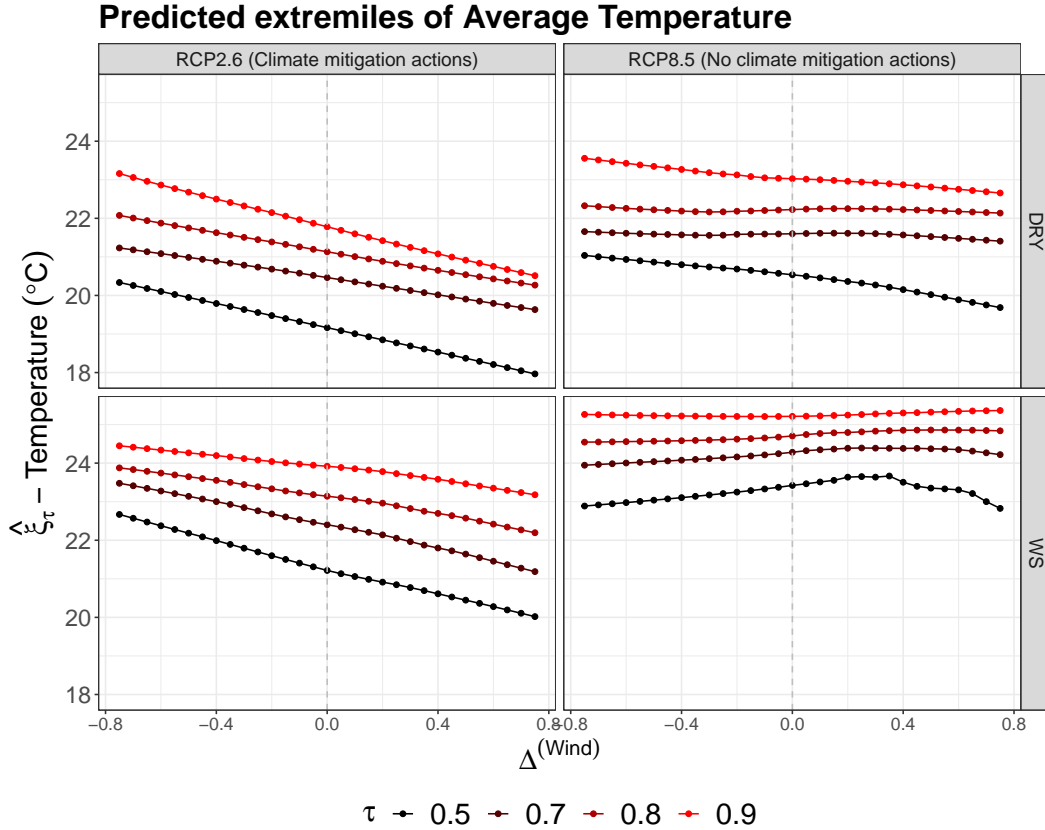


FIG 8. Predicted extremiles at levels  $\tau = 0.5, 0.7, 0.8, 0.9$  (in shades from black to red) of air temperature for shifts of the average wind speed of the month of July. For both reference year (first row) and warm summer (second row) cases, we show both RCP2.6 and RCP8.5 scenarios, in the first and second columns, respectively.

that global warming brings consequences that are far more complex than a simple overall increase in temperature or decrease in humidity. Notice that all scripts used to produce the analysis in this manuscript are available at <https://github.com/LauraBattagliola/Extremile-scalar-on-function-regression-with-application-to-climate-scenarios>.

Concerning further developments, our work offers several avenues for extensions. For instance, determining hyperparameter  $\kappa$ , which controls the trade-off between estimated bias and variance of conditional CDF estimator as discussed in Section 3.5, is an interesting non-trivial task. Since  $\kappa$  is involved in the local bandwidth selection, it plays a crucial role in preventing estimated extremiles from crossing. In Figure 10 we compare the MSE of the estimated extremiles in our simulation study for different values of  $\kappa$ , and the difference is minimal. However, in the application we used different values of the hyperparameter in Sections 5.2 and 5.3 in order to avoid extremile crossing. A thorough analysis should then be dedicated to the automatized selection of such hyperparameter, taking into account its repercussions into the goodness-of-fit of the regression model.

Moreover, more complex functional models could be adapted to extremile regression. For instance, function-on-function models, where both responses and covariates are functions, and scalar-on-function mixed effects models for clustered or longitudinal data. These extensions would be particularly suitable for climate applications, as all recordings are inherently functional and data could be aggregated as long as month-specific and scenario-specific effects were into place. Notice that such models are already implemented in the context of

quantile regression (see for instance [Beyaztas, Shang and Alin \(2022\)](#) and [Battagliola et al. \(2024\)](#)), and it would be worthwhile to compare them to the corresponding extremile regression models, as was done in Section 4.

Finally, it would be of great interest to extend the conditional extremile estimator to extreme levels  $\tau \uparrow 1$  and  $\tau \downarrow 0$ , as done by [Daouia, Gijbels and Stupfler \(2022\)](#) in the case of multivariate covariates. Such extension to functional covariates, done by [Gardes and Girard \(2012\)](#) in the case of quantile scalar-on-function regression, needs to be handled with care, as operating with the distributions of functional random elements requires special mathematical care. In terms of threshold selection, methods from [Bladt, Albrecher and Beirlant \(2020\)](#) could be useful in the functional setting. Nevertheless, given the amount of applications that can be represented via functional data, such methodology would be highly valuable. This could lead to more robust statistical models that are capable of dealing with extremes, not least for climate applications.

**Funding.** The first author was partly funded by European Research Council under Grant CoG 2015-682172NETS, within the Seventh European Union Framework Program. The second author was supported by the Carlsberg Foundation, grant number CF23-1096.

## APPENDIX A: PROOFS

**A.1. Notation for proofs.** We keep part of the notation similar to the one of [Ferraty and Nagy \(2021\)](#) in order to make comparisons with their work straightforward.

In the following, we list the terms that appear in [Lemmas A.1 and A.3](#), and [Corollary A.4](#):

$$\begin{aligned}
& X(\cdot) \in E \text{ is a function drawn from the distribution of } X(\cdot) \\
& \pi_x(h) = \mathbb{P}(\|X - x\| \leq h), \text{ is continuous in a neighborhood of } 0. \\
& \vartheta_x(u) = \lim_{h \downarrow 0} \frac{\pi_x(uh)}{\pi_x(h)}, \text{ for all } u > 0 \\
& \gamma_{j_1, \dots, j_K}^{p_1, \dots, p_K}(t) = \mathbb{E} \left[ \prod_{k=1}^K \langle \phi_{j_k}, X - x \rangle^{p_k} \middle| \|X - x\|^{\sum_k p_k} = t \right] \\
& \tilde{\gamma}_{j_1, \dots, j_K}^{p_1, \dots, p_K}(t) = \frac{d}{dt} \gamma_{j_1, \dots, j_K}^{p_1, \dots, p_K}(t) \\
& [\Gamma]_{j_1, j_2} = \tilde{\gamma}_{j_1, j_2}^{1,1}(0) \\
& \sigma^2(x) = \text{Var}(Y|X = x) \\
& \alpha_\tau^1(0|x, K) = \sum_{k > K} \langle \phi_k, \xi'_{\tau, x} \rangle \tilde{\gamma}_k^1(0) \\
& \alpha_\tau^1(j|x, K) = \sum_{k > K} \langle \phi_k, \xi'_{\tau, x} \rangle \tilde{\gamma}_{j, k}^{1,1}(0) \\
& \alpha_\tau^2(j|x, K) = \sum_{k_1, k_2 > K} \langle \phi_{k_1}, \xi'_{\tau, x} \rangle \langle \phi_{k_2}, \xi'_{\tau, x} \rangle \tilde{\gamma}_{j, k_1, k_2}^{2,1,1}(0) \\
& \beta_\tau^1(0|x) = \sum_{k_1, k_2 > 0} \langle \xi''_{\tau, x} \phi_{k_1}, \phi_{k_2} \rangle \tilde{\gamma}_{k_1, k_2}^{1,1}(0) \\
& \beta_\tau^1(j|x) = \sum_{k_1, k_2 > 0} \langle \xi''_{\tau, x} \phi_{k_1}, \phi_{k_2} \rangle \tilde{\gamma}_{j, k_1, k_2}^{1,1,1}(0) \\
& \beta_\tau^2(0|x) = \sum_{k_1, k_2, k_3, k_4 > 0} \langle \xi''_{\tau, x} \phi_{k_1}, \phi_{k_2} \rangle \langle \xi''_{\tau, x} \phi_{k_3}, \phi_{k_4} \rangle \tilde{\gamma}_{k_1, k_2, k_3, k_4}^{1,1,1,1}(0) \\
& \beta_\tau^2(j|x) = \sum_{k_1, k_2, k_3, k_4 > 0} \langle \xi''_{\tau, x} \phi_{k_1}, \phi_{k_2} \rangle \langle \xi''_{\tau, x} \phi_{k_3}, \phi_{k_4} \rangle \tilde{\gamma}_{j, k_1, k_2, k_3, k_4}^{2,1,1,1,1}(0).
\end{aligned}$$

*Global bandwidth.* [Lemma A.5](#) involves the terms

$$\begin{aligned}
\delta_{\tau,0} &= \frac{\sum_{i=1}^n J_\tau(F(Y_i|x))L(h^{-1}\|X_i - x\|)}{n\mathbb{E}[J_\tau(F(Y_1|x))L(h^{-1}\|X_1 - x\|)]} \\
\delta_{\tau,j} &= \frac{\sum_{i=1}^n \langle \phi_j, X_i - x \rangle J_\tau(F(Y_i|x))L(h^{-1}\|X_i - x\|)}{n\mathbb{E}[J_\tau(F(Y_1|x))L(h^{-1}\|X_1 - x\|)]} \\
[\Delta_\tau]_{j_1, j_2} &= \frac{\sum_{i=1}^n \langle \phi_{j_1}, X_i - x \rangle \langle \phi_{j_2}, X_i - x \rangle J_\tau(F(Y_i|x))L(h^{-1}\|X_i - x\|)}{n\mathbb{E}[J_\tau(F(Y_1|x))L(h^{-1}\|X_1 - x\|)]} \\
A_{\tau,0} &= \frac{\sum_{i=1}^n \langle \mathcal{P}_K^\perp \xi'_{\tau, x}, X_i - x \rangle L(h^{-1}\|X_i - x\|)}{n\mathbb{E}[L(h^{-1}\|X_1 - x\|)]}
\end{aligned}$$

$$\begin{aligned}
A_{\tau,j} &= \frac{\sum_{i=1}^n \langle \mathcal{P}_K^\perp \xi'_{\tau,x}, X_i - x \rangle \langle \phi_j, X_i - x \rangle L(h^{-1} \|X_i - x\|)}{n \mathbb{E}[L(h^{-1} \|X_1 - x\|)]} \\
B_{\tau,0} &= \frac{\sum_{i=1}^n R_{\tau,x,x,i} L(h^{-1} \|X_i - x\|)}{n \mathbb{E}[L(h^{-1} \|X_1 - x\|)]} \\
B_{\tau,j} &= \frac{\sum_{i=1}^n R_{\tau,x,x,i} \langle \phi_j, X_i - x \rangle L(h^{-1} \|X_i - x\|)}{n \mathbb{E}[L(h^{-1} \|X_1 - x\|)]} \\
C_{\tau,0} &= \frac{\sum_{i=1}^n (R_{\tau,\rho,x,i} - R_{\tau,x,x,i}) L(h^{-1} \|X_i - x\|)}{n \mathbb{E}[L(h^{-1} \|X_1 - x\|)]} \\
C_{\tau,j} &= \frac{\sum_{i=1}^n (R_{\tau,\rho,x,i} - R_{\tau,x,x,i}) \langle \phi_j, X_i - x \rangle L(h^{-1} \|X_i - x\|)}{n \mathbb{E}[L(h^{-1} \|X_1 - x\|)]},
\end{aligned}$$

and additional terms in proof on Theorem 3.2 are

$$\begin{aligned}
\delta_0 &= \frac{\sum_{i=1}^n (L(h^{-1} \|X_i - x\|))^2}{(n \mathbb{E}[L(h^{-1} \|X_1 - x\|)])^2} \\
\delta_j &= \frac{\sum_{i=1}^n \langle \phi_j, X_i - x \rangle (L(h^{-1} \|X_i - x\|))^2}{(n \mathbb{E}[L(h^{-1} \|X_1 - x\|)])^2} \\
[\Delta]_{j_1, j_2} &= \frac{\sum_{i=1}^n \langle \phi_{j_1}, X_i - x \rangle \langle \phi_{j_2}, X_i - x \rangle (L(h^{-1} \|X_i - x\|))^2}{(n \mathbb{E}[L(h^{-1} \|X_1 - x\|)])^2}.
\end{aligned}$$

*Local bandwidth.* Lemma A.10 and Theorem 3.3 involve

$$\begin{aligned}
\delta_{\tau,0}^\ell &= \frac{\sum_{i=1}^n J_\tau(F(Y_i|x)) L((h_i^k)^{-1} \|X_i - x\|)}{n \mathbb{E}[J_\tau(F(Y|x)) L((h_1^k)^{-1} \|X_1 - x\|)]} \\
\delta_{\tau,j}^\ell &= \frac{\sum_{i=1}^n \langle \phi_j, X_i - x \rangle J_\tau(F(Y_i|x)) L((h_i^k)^{-1} \|X_i - x\|)}{n \mathbb{E}[J_\tau(F(Y|x)) L((h_1^k)^{-1} \|X_1 - x\|)]} \\
[\Delta_\tau^\ell]_{j_1, j_2} &= \frac{\sum_{i=1}^n \langle \phi_{j_1}, X_i - x \rangle \langle \phi_{j_2}, X_i - x \rangle J_\tau(F(Y_i|x)) L((h_i^k)^{-1} \|X_i - x\|)}{n \mathbb{E}[J_\tau(F(Y|x)) L((h_1^k)^{-1} \|X_1 - x\|)]} \\
A_{\tau,0}^\ell &= \frac{\sum_{i=1}^n \langle \mathcal{P}_K^\perp \xi'_{\tau,x}, X_i - x \rangle L((h_i^k)^{-1} \|X_i - x\|)}{n \mathbb{E}[L((h_1^k)^{-1} \|X_1 - x\|)]} \\
A_{\tau,j}^\ell &= \frac{\sum_{i=1}^n \langle \mathcal{P}_K^\perp \xi'_{\tau,x}, X_i - x \rangle \langle \phi_j, X_i - x \rangle L((h_i^k)^{-1} \|X_i - x\|)}{n \mathbb{E}[L((h_1^k)^{-1} \|X_1 - x\|)]} \\
B_{\tau,0}^\ell &= \frac{\sum_{i=1}^n R_{\tau,x,x,i} L((h_i^k)^{-1} \|X_i - x\|)}{n \mathbb{E}[L((h_1^k)^{-1} \|X_1 - x\|)]} \\
B_{\tau,j}^\ell &= \frac{\sum_{i=1}^n R_{\tau,x,x,i} \langle \phi_j, X_i - x \rangle L((h_i^k)^{-1} \|X_i - x\|)}{n \mathbb{E}[L((h_1^k)^{-1} \|X_1 - x\|)]}.
\end{aligned}$$

## A.2. Assumptions.

*Local linear scalar-on-function regression.* The following are the assumptions from [Feraty and Nagy \(2021\)](#), adapted to the local linear extremile regression.

(A1) For any  $u$  in the neighborhood of  $0 \in E$ , there exists  $\nu = x + tu$ , with  $t \in (0, 1)$ , such that, for fixed  $\tau \in (0, 1)$

$$\xi_\tau(x + u) = \xi_\tau(x) + \langle \xi'_{\tau,x}, u \rangle + \frac{1}{2} \langle \xi''_{\tau,\nu} u, u \rangle,$$

with extremile regression operator  $\xi_\tau : E \rightarrow \mathbb{R}$ , its functional derivative  $\xi'_{\tau,x} : E \rightarrow E$  and  $\xi''_{\tau,\nu} : E \rightarrow E$  is a Hilbert–Schmidt linear operator such that there exists  $C \leq 0$  for which  $d(\xi''_{\tau,\nu_1}, \xi''_{\tau,\nu_2}) \leq Cd(\nu_1, \nu_2)$  for any  $\nu_1(\cdot), \nu_2(\cdot)$  in the neighborhood of  $x(\cdot) \in E$ .

(A2) The kernel function  $L$  is continuously differentiable on its support  $(0, 1)$  with  $L'(s) \leq 0$  for all  $s \in (0, 1)$  and  $L(1) > 0$ .

(A3) The functions  $\gamma_{j_1}^1, \gamma_{j_1, j_2}^{1,1}, \dots, \gamma_{j_1, j_2, j_3, j_4}^{1,1,1,1}, \gamma_{j_1}^2, \gamma_{j_1, j_2, j_3}^{2,1,1}, \dots, \gamma_{j_1, j_2, j_3, j_4, j_5}^{2,1,1,1,1}, \gamma_{j_1, j_2}^{2,2}$  are continuously differentiable around 0. The smallest eigenvalue of  $\Gamma$ , denoted  $\lambda_K$ , is strictly positive.

(A4) The bandwidth sequence  $h = h_n$  is such that as  $n \rightarrow \infty$  we have  $h_n \rightarrow 0$ ; The number of basis functions used  $K = K_n$  is such that  $K_n \rightarrow \infty$  and  $n\pi_x(h) \rightarrow \infty$ . Finally,  $h\sqrt{K} = o(1)$ ,  $\frac{1}{h\lambda_K\sqrt{n\pi_x(h)}} = o(1)$  and  $\frac{\sqrt{K}}{h\sqrt{\lambda_K n\pi_x(h)}} = o(1)$ .

(A5) For any  $s > 0$ ,  $\frac{\pi_x(sh)}{\pi_x(h)} \rightarrow \theta_x(s)$  as  $h \rightarrow 0$ .

(A6) For fixed  $\tau \in (0, 1)$ , operator  $\sigma_\tau^2(x) = \text{Var}(J_\tau(F(Y|X))Y|X = x)$  is uniformly continuous.

(A7)  $h \mapsto \pi_x(h)$  is a continuous function in the neighborhood of 0 such that  $\theta_x(s) \geq s$  and  $\theta_x(s^{-1}) \leq s^{-1} \forall s > 1$ ; moreover, the number of neighbours in the kNN algorithm  $k = k_n$  is such that  $\frac{k}{n} = o(1)$ ,  $\frac{\sqrt{K}}{\pi_x(\frac{k}{n})} = o(1)$ ,  $\frac{1}{\pi_x(\frac{k}{n})\lambda_K\sqrt{k}} = o(1)$ , and  $\frac{\sqrt{\lambda_K}}{\pi_x(\frac{k}{n})\sqrt{Kk}} = o(1)$ , with  $K = K_n \rightarrow \infty$  as  $n \rightarrow \infty$ .

*Uniform consistency of conditional cumulative distribution function estimator.* We rely on the assumption from [Ferraty et al. \(2010\)](#), and we re-state them here for completeness.

Define the subspaces  $\mathcal{S}_x \subset E$  and  $\mathcal{S}_y \subset \mathbb{R}$ , and the open ball  $B_r(x) = \{\tilde{x} \in E : d(x, \tilde{x}) \leq r\}$ . Two functions are key components in this framework:  $\varphi$ , controlling the concentration of probability measure of functional random variable  $X$  on  $B_r(x)$ , and  $\psi_{\mathcal{S}}(\epsilon)$ , Kolmogorov's  $\epsilon$ -entropy of a set  $\mathcal{S} \subset E$ . In particular, the latter is defined as the minimal number of open balls of radius  $\epsilon$  needed to cover  $\mathcal{S}$ . Intuitively, the lower  $\psi_{\mathcal{S}}(\epsilon)$ , the less complex the topological structure of  $\mathcal{S}$ .

Now consider kernel  $L_F$  with bandwidth  $h_F$  such that  $h_F = h_{F,n} \rightarrow 0$  with  $n \rightarrow \infty$ . Consider the following assumptions.

(A8) For all  $(y_1, y_2) \in \mathcal{S}_y \times \mathcal{S}_y$ , and all  $(x_1, x_2) \in \mathcal{S}_x \times \mathcal{S}_x$

$$|F(y_1|x_1) - F(y_2|x_2)| \leq C(d(x_1, x_2)^{b_x} + |y_1 - y_2|^{b_y}),$$

with  $C, b_x, b_y > 0$ .

(A9) The functions  $\varphi$  and  $\psi_{\mathcal{S}_x}$  are such that

- There exist  $C > 0$ , and  $\eta_0 > 0$ , s.t. for all  $\eta < \eta_0$

$$\left. \frac{d}{dt} \varphi(t) \right|_{\eta} < C.$$

Additionally, if  $L^F(1) = 0$ : there exist  $C > 0$ , and  $\eta_0 > 0$ , s.t. for all  $0 < \eta < \eta_0$

$$\int_0^\eta \varphi(u) du > C\eta\varphi(\eta).$$

- For  $n$  large enough:

$$\frac{(\log n)^2}{n\varphi(h_F)} < \psi_{\mathcal{S}_x} \left( \frac{\log n}{n} \right) < \frac{n\varphi(h_F)}{\log n}.$$

(A10)  $\forall x \in \mathcal{S}_x$

$$0 < C\varphi(h) \leq \mathbb{P}(X \in B_r(x)) \leq C'\varphi(h) < \infty,$$

with  $C, C' > 0$ .

(A11)  $L_F$  is a bounded and Lipschitz kernel on its support  $[0, 1)$ , and if  $L_F(1) = 0$ , the kernel  $L_F(1)$  fulfills the additional condition  $-\infty < C < \frac{d}{dt}L_F(t) < C' < 0$ , with  $C, C' > 0$ .

(A12) For some  $\beta > 1$ , Kolmogorov's  $\varepsilon$ -entropy of  $\mathcal{S}_x$  satisfies

$$\sum_{n=1}^{\infty} n^{\frac{1}{2\beta}} e^{(1-\beta)\psi_{\mathcal{S}_x}(\frac{\log n}{n})} < \infty.$$

It was shown in [Ferraty et al. \(2010\)](#) that, under assumptions (A8) – (A12), the estimator

$$\hat{F}_{h_F}(y|x) = \frac{\sum_{i=1}^n L_F(h_F^{-1}\|x - X_i\|) 1(Y_i \leq y)}{\sum_{i=1}^n L_F(h_F^{-1}\|x - X_i\|)}, \quad \forall y \in \mathbb{R}, \forall x \in E,$$

is uniformly consistent. In particular, for  $\mathcal{S}_x \subset E$  and  $\mathcal{S}_y \subset \mathbb{R}$

$$\sup_{x \in \mathcal{S}_x} \sup_{y \in \mathcal{S}_y} |F(y|x) - \hat{F}_{h_F}(y|x)| \rightarrow 0 \text{ a.s.}$$

**A.3. Technical lemmas.** This section is dedicated to stating and proving the technical lemmas involved in the proofs in Section A.4. Notice that Lemmas A.1 and A.8 are pivotal to generalize the local linear scalar-on-functional regression to the weighted version we propose. The rest of the results follow from the said lemmas and further results in the supplementary of [Ferraty and Nagy \(2021\)](#). Finally, Lemma A.7 corresponds to Lemma S.5 of [Ferraty and Nagy \(2021\)](#) and we add it here for completeness.

*Global bandwidth.*

LEMMA A.1. For  $i = 1, \dots, n$ ,  $p \geq 0$ ,  $q > 0$ , and  $\tau \in (0, 1)$ , we have

$$\int_{\mathbb{R}} \int_0^1 t^p \left[ L(t) J_{\tau}(\hat{F}_{h_F}(y|x)) \right]^q dF_{\|X_i - x\|/h}(t) dF_Y(y) = C_{\tau}(p, q|x) \pi_x(h) (1 + o(1)),$$

where  $C_{\tau}(p, q|x) = \mathbb{E}[J_{\tau}(F(Y|x))^q] \left\{ L^q(1) - \int_0^1 \frac{d}{du}(u^p L^q(u)) \vartheta_x(u) du \right\}$ .

PROOF. For  $\tau \in (0, 1/2]$ , define  $R_{s(\tau)}(y) = \frac{(1 - \hat{F}_{h_F}(y|x))^{s(\tau)-1}}{(1 - F(y|x))^{s(\tau)-1}}$ . Then  $R_{s(\tau)} \rightarrow 1$  uniformly almost surely by Theorem 4 of [Ferraty et al. \(2010\)](#) and so it may be seen that using the convergence result of Lemma S8 in [Ferraty and Nagy \(2021\)](#) we readily obtain

$$\begin{aligned} & \int_{\mathbb{R}} \int_0^1 t^p \left[ L(t) s(\tau) (1 - \hat{F}_{h_F}(y|x))^{s(\tau)-1} \right]^q dF_{\|X_i - x\|/h}(t) dF_Y(y) \\ &= s(\tau)^q \left[ \int_0^1 t^p L(t)^q dF_{\|X_i - x\|/h}(t) \right] \int_{\mathbb{R}} (1 - \hat{F}_{h_F}(y|x))^{q(s(\tau)-1)} dF_Y(y) \\ &= s(\tau)^q \left[ \int_0^1 t^p L(t)^q dF_{\|X_i - x\|/h}(t) \right] \int_{\mathbb{R}} (R_{s(\tau)}(y) (1 - F(y|x)))^{q(s(\tau)-1)} dF_Y(y) \end{aligned}$$

$$\begin{aligned}
&= s(\tau)^q \left[ \int_0^1 t^p L(t)^q dF_{\|X_i - x\|/h}(t) \right] \mathbb{E} \left[ (R_{s(\tau)}(y)(1 - F(y|x)))^{q(s(\tau)-1)} \right] \\
&= s(\tau)^q \left[ \int_0^1 t^p L(t)^q dF_{\|X_i - x\|/h}(t) \right] \mathbb{E} \left[ ((1 - F(y|x)))^{q(s(\tau)-1)} \right] (1 + o(1)) \\
&= C_\tau(p, q|x) \pi_x(h) (1 + o(1)),
\end{aligned}$$

where  $C_\tau(p, q|x) = \mathbb{E} [s(\tau)^q (1 - F(Y|x))^{q(s(\tau)-1)}] \left\{ L^q(1) - \int_0^1 \frac{d}{du} (u^p L^q(u)) \vartheta_x(u) du \right\}$ .

With similar arguments, the result holds for  $\tau \in [1/2, 1)$  with the constant  $C_\tau(p, q|x) = \mathbb{E} [r(\tau)^q F(Y|x)^{q(r(\tau)-1)}] \left\{ L^q(1) - \int_0^1 \frac{d}{du} (u^p L^q(u)) \vartheta_x(u) du \right\}$ . Collecting the constants proves the result.  $\square$

**COROLLARY A.2.** *For any  $q > 0$*

$$\mathbb{E}[(L(h^{-1}\|x - X\|))^q] = C_{0.5}(x|0, q) \pi_x(h) \{1 + o(1)\}.$$

**PROOF.** The result follows from  $J_{0.5}(F(y|x)) = 1$ .  $\square$

**LEMMA A.3.** *We have that*

1. *For any  $q > 0$*

$$\begin{aligned}
&\mathbb{E}[(L(h^{-1}(x - X)))^q J_\tau(\hat{F}_{h_F}(Y|x)) \gamma_{j_1, \dots, j_K}^{p_1, \dots, p_K} (\|X - x\|^p)] \\
&= h^p C_\tau(p, q|x) \tilde{\gamma}_{j_1, \dots, j_K}^{p_1, \dots, p_K}(0) \pi_x(h) (1 + o(1)),
\end{aligned}$$

with  $p = \sum_{k=1}^K p_k$ .

2. *All the following sums are smaller or equal to 1:*

$$\begin{aligned}
&\sum_j (\tilde{\gamma}_j^1(0))^2, \quad \sum_{j_1, j_2} (\tilde{\gamma}_{j_1, j_2}^{1,1}(0))^2, \quad \sum_{j_1, j_2, j_3} (\tilde{\gamma}_{j_1, j_2, j_3}^{1,1,1}(0))^2, \\
&\sum_{j_1, j_2, j_3, j_4} (\tilde{\gamma}_{j_1, j_2, j_3, j_4}^{1,1,1,1}(0))^2, \quad \sum_j \tilde{\gamma}_j^2(0), \quad \sum_{j_1, j_2} \tilde{\gamma}_{j_1, j_2}^{2,2}(0).
\end{aligned}$$

3.  $\Gamma$  is positive semidefinite.

**PROOF.** Using the adapted Lemma A.1, the rest of the proof is analogous to (Ferraty and Nagy, 2021, Lemma S.9).  $\square$

**COROLLARY A.4.** *The following holds*

$$\begin{aligned}
|\alpha_\tau^1(0|x, K)| &\leq \|\mathcal{P}_K^\perp \xi'_\tau\|, \quad \sum_{k=1}^K (\alpha_\tau^1(k|x, K))^2 \leq \|\mathcal{P}_K^\perp \xi'_\tau\|^2, \quad \sum_{k=1}^K \alpha_\tau^2(k|x, K) \leq \|\mathcal{P}_K^\perp \xi'_\tau\|^2 \\
\beta_\tau^1(0, x) &= \mathcal{O}(1), \quad \sum_{k=1}^K (\beta_\tau^1(k, x))^2 = \mathcal{O}(1), \quad \sum_{k=1}^K \beta_\tau^2(k, x) = \mathcal{O}(1).
\end{aligned}$$

**PROOF.** Follows from Lemma A.3 and the Cauchy-Schwartz inequality.  $\square$

**LEMMA A.5.** *Under the hypothesis (A1) – (A5)*

1. For all  $j, j_1, j_2 = 1, \dots, K$

$$\begin{aligned}\delta_{\tau,j} &= \frac{C_\tau(1, 1|x)}{C_\tau(0, 1|x)} \tilde{\gamma}_j^1(0) h \{1 + o_{\mathbb{P}}(1)\} + \mathcal{O}_{\mathbb{P}}(h \{n\pi_x(h)\}^{-1/2}) \sqrt{\tilde{\gamma}_j^2(0)} \\ [\Delta_\tau]_{j_1, j_2} &= \frac{C_\tau(2, 1|x)}{C_\tau(0, 1|x)} \tilde{\gamma}_{j_1, j_2}^{1,1}(0) h^2 \{1 + o_{\mathbb{P}}(1)\} + \mathcal{O}_{\mathbb{P}}(h^2 \{n\pi_x(h)\}^{-1/2}) \sqrt{\tilde{\gamma}_{j_1, j_2}^{2,2}(0)}\end{aligned}$$

2. For all  $j = 1, \dots, K$

$$\begin{aligned}A_{\tau,0} &= \frac{C_\tau(1, 1|x)}{C_\tau(0, 1|x)} \alpha_\tau^1(0|x, K) h \{1 + o(1)\} + \mathcal{O}_{\mathbb{P}}(\|\mathcal{P}_K^\perp \xi'_{\tau,x}\| h \{n\pi_x(h)\}^{-1/2}) \\ A_{\tau,j} &= \frac{C_\tau(2, 1|x)}{C_\tau(0, 1|x)} \alpha_\tau^1(j|x, K) h^2 \{1 + o(1)\} + \mathcal{O}_{\mathbb{P}}(\sqrt{\alpha_\tau^2(j|x, K)} h^2 \{n\pi_x(h)\}^{-1/2})\end{aligned}$$

3. For any  $\mathbf{u}, \mathbf{v} \in \mathbb{R}^K$ ,  $|\mathbf{u}^T \Gamma^{-1} \mathbf{v}| \leq \lambda_K^{-1} \|\mathbf{u}\|_2 \|\mathbf{v}\|_2$ , where  $\lambda_K$  is the smallest eigenvalue of  $\Gamma$ .

4. For all  $j = 1, \dots, K$

$$\begin{aligned}B_{\tau,0} &= \frac{C_\tau(2, 1|x)}{C_\tau(0, 1|x)} \beta_\tau^1(0|x) h^2 \{1 + o(1)\} + \mathcal{O}_{\mathbb{P}}(h^2 \{n\pi_x(h)\}^{-1/2}) \\ B_{\tau,j} &= \frac{C_\tau(3, 1|x)}{C_\tau(0, 1|x)} \beta_\tau^1(j|x) h^3 \{1 + o(1)\} + \sqrt{\beta_\tau^2(j|x)} \mathcal{O}_{\mathbb{P}}(h^3 \{n\pi_x(h)\}^{-1/2})\end{aligned}$$

PROOF. Using Lemmas A.1 and A.3, the rest of the proof is analogous to (Ferraty and Nagy, 2021, Lemmas S.10 – S.14).  $\square$

LEMMA A.6. Under the hypothesis (A1) – (A5) and using Corollary A.2, for all  $j, j_1, j_2 = 1, \dots, K$

$$\begin{aligned}\delta_0 &= \frac{C_{0.5}(0, 2|x)}{(C_{0.5}(0, 1|x))^2} \{n\pi_x(h)\}^{-1} \{1 + o_{\mathbb{P}}(1)\} \\ \delta_j &= \frac{C_{0.5}(1, 2|x)}{(C_{0.5}(0, 1|x))^2} \tilde{\gamma}_j^1(0) h \{n\pi_x(h)\}^{-1} \{1 + o_{\mathbb{P}}(1)\} + \mathcal{O}_{\mathbb{P}}(h \{n\pi_x(h)\}^{-3/2}) \sqrt{\tilde{\gamma}_j^2(0)} \\ [\Delta]_{j_1, j_2} &= \frac{C_{0.5}(2, 2|x)}{(C_{0.5}(0, 1|x))^2} \tilde{\gamma}_{j_1, j_2}^{1,1}(0) h^2 \{n\pi_x(h)\}^{-1} \{1 + o_{\mathbb{P}}(1)\} + \mathcal{O}_{\mathbb{P}}(h^2 \{n\pi_x(h)\}^{-3/2}) \sqrt{\tilde{\gamma}_{j_1, j_2}^{2,2}(0)}.\end{aligned}$$

PROOF. Analogous to proof of 1. of Lemma A.5.  $\square$

Local bandwidth.

LEMMA A.7. Under (A7), a.s.

$$\pi_x(h^k) \sim \frac{k}{n}, \quad h^k \sim \pi_x^{-1} \left( \frac{k}{n} \right),$$

where  $h^k = \inf \left\{ h \in H : \sum_{j=1}^n \mathbf{1}_{X_j \in B_h(x)} = k \right\}$ .

PROOF. See proof of Lemma S.5 of Supplementary materials to Ferraty and Nagy (2021).  $\square$

LEMMA A.8. Under (A2), (A3), (A5) and (A7), for  $i = 1, \dots, n$ ,  $p \geq 0$ ,  $q > 0$ , and  $\tau \in (0, 1)$ , we have

$$\int_{\mathbb{R}} \int_0^1 t^p \left[ L(t) J_\tau(\hat{F}_{h_F}(y|x)) \right]^q dF_{\|X_i - x\|/h_i^k}(t) dF_Y(y) = C_\tau(p, q|x) \frac{k}{n} (1 + o(1))$$

where  $C_\tau(p, q|x)$  is defined in Lemma A.1.

PROOF. Consider  $\mathcal{S}_{-i} = \{X_1, \dots, X_{i-1}, X_{i+1}, \dots, X_n\}$  and write

$$\begin{aligned} & \mathbb{E}[(h_i^k)^{-1} \|X_i - x\|]^p L^q((h_i^k)^{-1} \|X_i - x\| | \mathcal{S}_{-i}) \\ &= L^q(1) - \int_0^1 \frac{d}{du} (u^p L^q(u)) \pi_x(h_i^k u) du \\ &= \pi_x(h_i^k) \left\{ L^q(1) - \int_0^1 \frac{d}{du} (u^p L^q(u)) \frac{\pi_x(h_i^k u)}{\pi_x(h_i^k)} du \right\} \\ &\sim \pi_x(h_i^k) \left\{ L^q(1) - \int_0^1 \frac{d}{du} (u^p L^q(u)) \theta_x(u) du \right\} \text{ a.s.,} \end{aligned}$$

where the last step comes from the fact that  $\sup_{s \in [0,1]} \left| \frac{\pi_x(h_i^k s)}{\pi_x(h_i^k)} - \theta_x(s) \right| \rightarrow 0$  almost surely (see proof of Lemma S.6-(i) in the Supplementary of Ferraty and Nagy (2021)). Thus, from Lemma A.7 and the law of total expectation, we have

$$\begin{aligned} & \mathbb{E}[(h_i^k)^{-1} \|X_i - x\|]^p L^q((h_i^k)^{-1} \|X_i - x\| | \mathcal{S}_{-i}) \\ &= \frac{k}{n} \left\{ L^q(1) - \int_0^1 \frac{d}{du} (u^p L^q(u)) \theta_x(u) du \right\} (1 + o(1)). \end{aligned}$$

Hence, similarly to the proof of Lemma A.1, we obtain the result

$$\begin{aligned} & \int_{\mathbb{R}} \int_0^1 t^p \left[ L(t) J_\tau(\hat{F}_{h_F}(y|x)) \right]^q dF_{\|X_i - x\|/h_i^k}(t) dF_Y(y) \\ &= C_\tau(p, q|x) \frac{k}{n} (1 + o(1)). \end{aligned}$$

□

LEMMA A.9. Under (A2), (A3), (A5) and (A7), for  $i = 1, \dots, n$ , for any  $q > 0$ , and  $\tau \in (0, 1)$ , we have

$$\begin{aligned} & \mathbb{E}[L^q((h_i^k)^{-1} (x - X)) J_\tau(\hat{F}_{h_F}(Y|x)) \gamma_{j_1, \dots, j_K}^{p_1, \dots, p_K} (\|X - x\|^p)] \\ &= \left( \pi_x^{-1} \left( \frac{k}{n} \right) \right)^p C_\tau(p, q|x) \tilde{\gamma}_{j_1, \dots, j_K}^{p_1, \dots, p_K}(0) \frac{k}{n} (1 + o(1)) \end{aligned}$$

with  $p = \sum_{k=1}^K p_k$ .

PROOF. Using Lemmas A.7 and A.8, the rest of the proof is analogous to (Ferraty and Nagy, 2021, Lemma S.9). □

LEMMA A.10. Under (A2), (A3), (A5) and (A7), for all  $j, j_1, j_2 = 1, \dots, K$  we have

$$\begin{aligned} \delta_{\tau,j}^\ell &= \frac{C_\tau(1,1|x)}{C_\tau(0,1|x)} \tilde{\gamma}_j^1(0) \pi_x^{-1} \left( \frac{k}{n} \right) \{1 + o_{\mathbb{P}}(1)\} + \mathcal{O}_{\mathbb{P}} \left( \pi_x^{-1} \left( \frac{k}{n} \right) k^{-1/2} \right) \sqrt{\tilde{\gamma}_j^2(0)} \\ [\Delta_\tau^\ell]_{j_1,j_2} &= \frac{C_\tau(2,1|x)}{C_\tau(0,1|x)} \tilde{\gamma}_{j_1,j_2}^{1,1}(0) \left( \pi_x^{-1} \left( \frac{k}{n} \right) \right)^2 \{1 + o_{\mathbb{P}}(1)\} + \mathcal{O}_{\mathbb{P}} \left( \left( \pi_x^{-1} \left( \frac{k}{n} \right) \right)^2 k^{-1/2} \right) \sqrt{\tilde{\gamma}_{j_1,j_2}^{2,2}(0)} \\ A_{\tau,0}^\ell &= \frac{C_\tau(1,1|x)}{C_\tau(0,1|x)} \omega_\tau^1(0|x, K) \pi_x^{-1} \left( \frac{k}{n} \right) \{1 + o(1)\} + \mathcal{O}_{\mathbb{P}} \left( \|\mathcal{P}_K^\perp \xi'_{\tau,x}\| \pi_x^{-1} \left( \frac{k}{n} \right) k^{-1/2} \right) \\ A_{\tau,j}^\ell &= \frac{C_\tau(2,1|x)}{C_\tau(0,1|x)} \omega_\tau^1(j|x, K) \left( \pi_x^{-1} \left( \frac{k}{n} \right) \right)^2 \{1 + o(1)\} + \mathcal{O}_{\mathbb{P}} \left( \sqrt{\omega_\tau^2(j|x, K)} \left( \pi_x^{-1} \left( \frac{k}{n} \right) \right)^2 k^{-1/2} \right) \\ B_{\tau,0}^\ell &= \frac{C_\tau(2,1|x)}{C_\tau(0,1|x)} \beta_\tau^1(0|x) \left( \pi_x^{-1} \left( \frac{k}{n} \right) \right)^2 \{1 + o(1)\} + \mathcal{O}_{\mathbb{P}} \left( \left( \pi_x^{-1} \left( \frac{k}{n} \right) \right)^2 k^{-1/2} \right) \\ B_{\tau,j}^\ell &= \frac{C_\tau(3,1|x)}{C_\tau(0,1|x)} \beta_\tau^1(j|x) \left( \pi_x^{-1} \left( \frac{k}{n} \right) \right)^3 \{1 + o(1)\} + \sqrt{\beta_\tau^2(j|x)} \mathcal{O}_{\mathbb{P}} \left( \left( \pi_x^{-1} \left( \frac{k}{n} \right) \right)^3 k^{-1/2} \right). \end{aligned}$$

PROOF. Using Lemmas A.8 and A.9, the rest of the proof is analogous to (Ferraty and Nagy, 2021, Lemma S.10, S.11, S.12, S.14).  $\square$

**A.4. Proofs of main theorems.** In this section we extend the proofs by Ferraty and Nagy (2021) for local linear scalar-on-function regression to the extremile scalar-on-function regression. In particular, we provide the proofs for the asymptotic bias and variance expressions of the conditional extremile estimator.

PROOF OF THEOREM 3.1. We require checking the order of magnitude of (17) and (18).

1. First, we rewrite  $T_1$  as

$$T_1 = \mathbf{e}^T (\Phi^T \widetilde{\mathbf{W}}_\tau \Phi)^{-1} (A_{\tau,0}, A_{\tau,1}, \dots, A_{\tau,K})^T$$

with  $A_{\tau,0}$  and  $A_{\tau,j}$ ,  $j = 1, \dots, K$ , defined in Section A.1. The matrix to invert is  $\Phi^T \widetilde{\mathbf{W}}_\tau \Phi$ , where  $\widetilde{\mathbf{W}}_\tau = (n \mathbb{E}[J_\tau(F(Y|x))L(h^{-1}(x-X))])^{-1} \mathbf{W}_\tau$ . Hence we have that

$$(37) \quad \Phi^T \widetilde{\mathbf{W}}_\tau \Phi = \begin{bmatrix} \delta_{\tau,0} & \delta_\tau^T \\ \delta_\tau & \Delta_\tau \end{bmatrix},$$

with  $\delta_\tau = (\delta_{\tau,1}, \dots, \delta_{\tau,K})^T$  and  $\Delta$  denoting the  $K \times K$  matrix whose entries are defined in Section A.1. With the inversion of the block matrix (37) we get

$$(38) \quad (\Phi^T \widetilde{\mathbf{W}}_\tau \Phi)^{-1} = \begin{bmatrix} (\delta_{\tau,0} - \delta_\tau^T \Delta_\tau^{-1} \delta_\tau)^{-1} & -(\delta_{\tau,0} - \delta_\tau^T \Delta_\tau^{-1} \delta_\tau)^{-1} \delta_\tau^T \Delta_\tau^{-1} \\ -(\delta_{\tau,0} - \delta_\tau^T \Delta_\tau^{-1} \delta_\tau)^{-1} \Delta_\tau^{-1} \delta_\tau & (\delta_{\tau,0} - \delta_\tau^T \Delta_\tau^{-1} \delta_\tau)^{-1} \Delta_\tau^{-1} \delta_\tau \delta_\tau^T \Delta_\tau^{-1} \end{bmatrix},$$

and hence

$$T_1 = (\delta_{\tau,0} - \delta_\tau^T \Delta_\tau^{-1} \delta_\tau)^{-1} (A_{\tau,0} - \delta_\tau^T \Delta_\tau^{-1} (A_{\tau,1}, \dots, A_{\tau,K})^T).$$

One can see arguing as in (Ferraty and Nagy, 2021, Lemma S.1 (i)) and using Lemma A.5 that

$$(39) \quad \Delta_\tau^{-1} = \frac{C_\tau(0,1|x)}{C_\tau(2,1|x)} h^{-2} \Gamma^{-1} (1 + o_{\mathbb{P}}(1)),$$

where  $\Gamma$  is a  $K \times K$  defined in Section A.1. Then, as in (Ferraty and Nagy, 2021, Lemma S.1 (i)) and using Lemmas A.1, A.3 and A.5, as well as the upper bounds in Corollary A.4, we see that

$$(40) \quad (\delta_{\tau,0} - \delta_{\tau}^T \Delta_{\tau}^{-1} \delta_{\tau})^{-1} = \mathcal{O}_{\mathbb{P}}(\lambda_K)$$

$$(A_{\tau,0} - \delta_{\tau}^T \Delta_{\tau}^{-1} (A_{\tau,1}, \dots, A_{\tau,K})^T) = \mathcal{O}_{\mathbb{P}}(h \|\mathcal{P}_K^{\perp} \xi'_{\tau}\|) + \mathcal{O}_{\mathbb{P}}\left(\frac{h}{\sqrt{n\pi_x(h)}} \|\mathcal{P}_K^{\perp} \xi'_{\tau}\|\right)$$

$$- \mathcal{O}_{\mathbb{P}}(\lambda_K^{-1} h \|\mathcal{P}_K^{\perp} \xi'_{\tau}\|) + \mathcal{O}_{\mathbb{P}}\left(\lambda_K^{-1} \frac{h}{\sqrt{n\pi_x(h)}} \|\mathcal{P}_K^{\perp} \xi'_{\tau}\|\right).$$

Hence,  $T_1 = \mathcal{O}_{\mathbb{P}}(h \|\mathcal{P}_K^{\perp} \xi'_{\tau}\|)$ .

2. We rewrite  $T_2$  as

$$T_2 = \mathbf{e}^T (\Phi^T \widetilde{\mathbf{W}}_{\tau} \Phi)^{-1} [(B_{\tau,0}, B_{\tau,1}, \dots, B_{\tau,K})^T + (C_{\tau,0}, C_{\tau,1}, \dots, C_{\tau,K})^T],$$

and once again we use inverse matrix (38) to obtain

$$T_2 = (\delta_{\tau,0} - \delta_{\tau}^T \Delta_{\tau}^{-1} \delta_{\tau})^{-1} (B_{\tau,0} - \delta_{\tau}^T \Delta_{\tau}^{-1} (B_{\tau,1}, \dots, B_{\tau,K})^T)$$

$$+ (\delta_{\tau,0} - \delta_{\tau}^T \Delta_{\tau}^{-1} \delta_{\tau})^{-1} (C_{\tau,0} - \delta_{\tau}^T \Delta_{\tau}^{-1} (C_{\tau,1}, \dots, C_{\tau,K})^T).$$

Following similar arguments arguments to the ones used for  $T_1$ , with Lemmas A.1, A.3, A.5, and Corollary A.4, we have that

$$(B_{\tau,0} - \delta_{\tau}^T \Delta_{\tau}^{-1} (B_{\tau,1}, \dots, B_{\tau,K})^T)$$

$$= \mathcal{O}_{\mathbb{P}}(h^2) + \mathcal{O}_{\mathbb{P}}\left(\frac{h^2}{\sqrt{n\pi_x(h)}}\right) - \mathcal{O}_{\mathbb{P}}(\lambda_K^{-1} h^2) + \mathcal{O}_{\mathbb{P}}\left(\lambda_K^{-1} \frac{h^2}{\sqrt{n\pi_x(h)}}\right).$$

Moreover, thanks to (A1),  $C_{\tau,0} = \mathcal{O}_{\mathbb{P}}(h^3)$  and  $C_{\tau,j} = \mathcal{O}_{\mathbb{P}}(h^4)$ , for  $j = 1, \dots, K$ , hence  $(C_{\tau,0} - \delta_{\tau}^T \Delta_{\tau}^{-1} (C_{\tau,1}, \dots, C_{\tau,K})^T) = (1 - h \delta_{\tau}^T \Delta_{\tau}^{-1} (1, \dots, 1)^T) \mathcal{O}_{\mathbb{P}}(h^3)$ . Thanks to (39) we have that

$$\delta_{\tau}^T \Delta_{\tau}^{-1} (1, \dots, 1)^T \propto \frac{1}{h^2} \delta_{\tau}^T \Gamma^{-1} (1, \dots, 1)^T,$$

and thanks to point 3. of Lemma A.5, we obtain

$$|\delta_{\tau}^T \Gamma^{-1} (1, \dots, 1)^T| \leq \lambda_K^{-1} \sqrt{K} \|\delta_{\tau}\|_2.$$

Since  $\|\delta_{\tau}\|_2 = \mathcal{O}_{\mathbb{P}}(h)$  because of point 1. Lemma A.5, we finally obtain

$$(C_{\tau,0} - \delta_{\tau}^T \Delta_{\tau}^{-1} (C_{\tau,1}, \dots, C_{\tau,K})^T) = \mathcal{O}_{\mathbb{P}}(\lambda_K^{-1} \sqrt{K} h^3).$$

Using assumption  $h\sqrt{K} = o(1)$  in (A4), we finally get that  $T_2 = \mathcal{O}_{\mathbb{P}}(h^2) + o_{\mathbb{P}}(h^2)$ .

The two above points prove the desired result.  $\square$

PROOF OF THEOREM 3.2. First consider

$$(41) \quad \Phi^T \widetilde{\mathbf{W}}^2 \Phi = \begin{bmatrix} \delta_0 & \delta^T \\ \delta & \Delta \end{bmatrix},$$

where  $\delta = (\delta_1, \dots, \delta_K)^T$  and  $\Delta$  denoting the  $K \times K$  matrix whose entries are defined in Section A.1. We can then rewrite (20) as

$$(42) \quad \text{Var}(\hat{\alpha}_{\tau} | \mathbf{X})$$

$$= [\sigma_{\tau}^2(x) + o(1)] (\delta_{\tau,0} - \delta_{\tau}^T \Delta_{\tau}^{-1} \delta_{\tau})^{-2} (\delta_0 - \delta_{\tau}^T \Delta_{\tau}^{-1} \delta - \delta^T \Delta_{\tau}^{-1} \delta_{\tau} + \delta_{\tau}^T \Delta_{\tau}^{-1} \Delta \Delta_{\tau}^{-1} \delta_{\tau}).$$

From (40) we know that

$$(\delta_{\tau,0} - \delta_{\tau}^T \Delta_{\tau}^{-1} \delta_{\tau})^{-2} = \mathcal{O}_{\mathbb{P}}(\lambda_K^2),$$

and from Lemmas A.5 and A.6, we obtain

$$(\delta_0 - \delta_{\tau}^T \Delta_{\tau}^{-1} \delta - \delta^T \Delta_{\tau}^{-1} \delta_{\tau} + \delta_{\tau}^T \Delta_{\tau}^{-1} \Delta \Delta_{\tau}^{-1} \delta_{\tau}) = \mathcal{O}_{\mathbb{P}}\left(\frac{1}{n\pi_x(h)}\right) + \mathcal{O}_{\mathbb{P}}\left(\frac{\lambda_K^{-1}}{n\pi_x(h)}\right),$$

proving the result.  $\square$

PROOF OF THEOREM 3.3. Using Lemmas A.8, A.9 and A.10, the proof is obtained similarly to the one of Theorems 3.1 and 3.2.  $\square$

## APPENDIX B: ADDITIONAL RESULTS

In this section we provide additional results corresponding to Sections 4 and 5.

As discussed in Section 1, extremiles fundamentally differ from other estimators, like quantiles. In order to illustrate this difference, we display in Figure 9 the estimated conditional extremiles and quantiles at the same levels. To do so, we use a simulated sample  $\{X_i(\cdot)\}_i$  as for our simulation study and impose different levels of heteroskedasticity. Then, we predict the extremiles and quantiles for regular shifts  $\Delta = [-1, \dots, 0, \dots, 1]$  of the point-wise average of the sample, i.e.  $AvgX(s) = \frac{1}{200} \sum_{i=1}^n X_i(s)$ , similarly to what we did in Section 5.3. The predicted quantiles were computed with R package `qgam` (Fasiolo et al., 2021). We see that, as  $\gamma$  grows, quantiles and extremiles are more different.

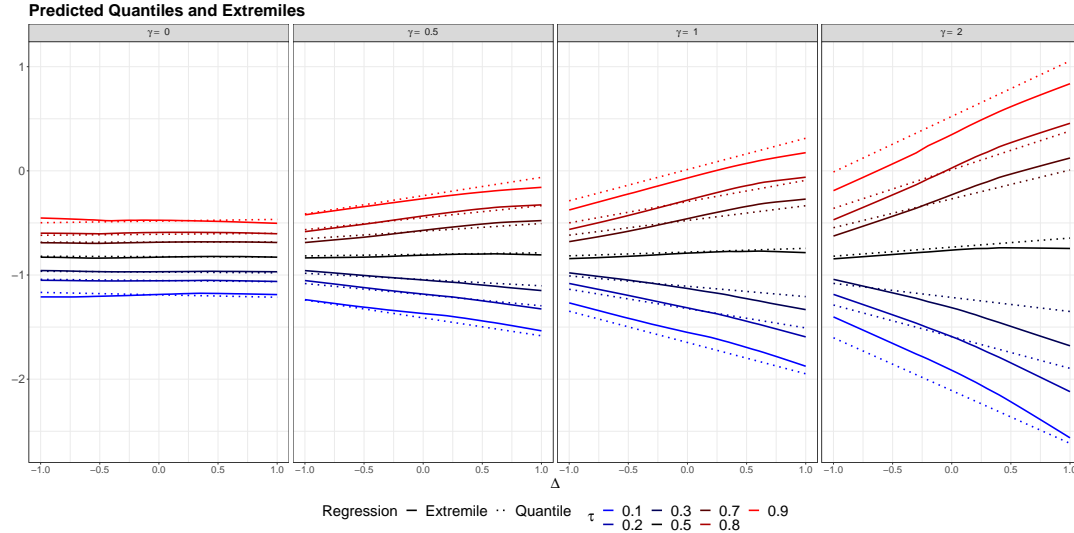


FIG 9. Predicted conditional extremiles (solid lines) and quantiles (dotted lines) for a simulated sample. We show the results for levels  $\tau = 0.1, 0.2, 0.3, 0.5, 0.7, 0.8, 0.9$  (from blue to red) and for heteroskedasticity level  $\gamma = 0, 0.5, 1, 2$  from first to fourth panel, respectively.

Moreover, in our simulation study we compared our results for the estimated extremiles at level  $\tau = 0.5$  with the estimated local linear means from package `flr`. In particular, to measure the difference between the estimated quantities we compute

$$D^{\gamma} = \frac{1}{B} \sum_{b=1}^B \frac{1}{n} \sum_{i=1}^n |\hat{\xi}_{0.5,b}^{\gamma}(X_i) - \hat{m}_b^{\gamma}(X_i)|,$$

where we denote with  $\widehat{m}_b^\gamma$  the mean estimator at iteration  $b$  in a simulation setting with heteroskedasticity level  $\gamma$ . In Table 3 we show such values. As expected the estimated quantities are very close to each other, even though they are not identical. This is due to the fact that our implementation relies on different linear algebra libraries than those of `f11r`.

TABLE 3  
Overall difference between estimated extremiles at level 0.5 and local linear mean for every value of  $\gamma$ .

	$\gamma = 0$	$\gamma = 0.5$	$\gamma = 1$	$\gamma = 2$
$D^\gamma$	2.9e-11	5.73e-11	9.88e-11	9.39e-11

Finally, we compare boxplots of MSE (34) for different values of hyperparameter  $\kappa$  in Figure 10. We plot the same values of Figure 2, namely those corresponding to  $\kappa = 1$ , in solid line, and those corresponding to  $\kappa = 0.5$  and  $\kappa = 4$  in dotted and dashed lines, respectively. We see that the difference between them is minimal. In particular, we measured the maximum across extremile levels of the average across observations and simulations of absolute difference between the results for  $\kappa = 1$ , i.e. the same value used in Section 4, and the other two values of  $\kappa$ . Such average is exactly 0 for both  $\kappa = 0.5, 4$  when  $\gamma = 0$ . This is the same in the scenario where  $\gamma = 0.5$  and for  $\kappa = 4$ , while for  $\kappa = 0.5$  is of the order of  $10^{-6}$ . For both  $\gamma = 1, 2$ , the difference between estimated extremiles with  $\kappa = 1$  and  $\kappa = 0.5$  is of the order of  $10^{-4}$ , while between results of estimation carried out with  $\kappa = 1$  and  $\kappa = 4$  is of the order of  $10^{-5}$ .

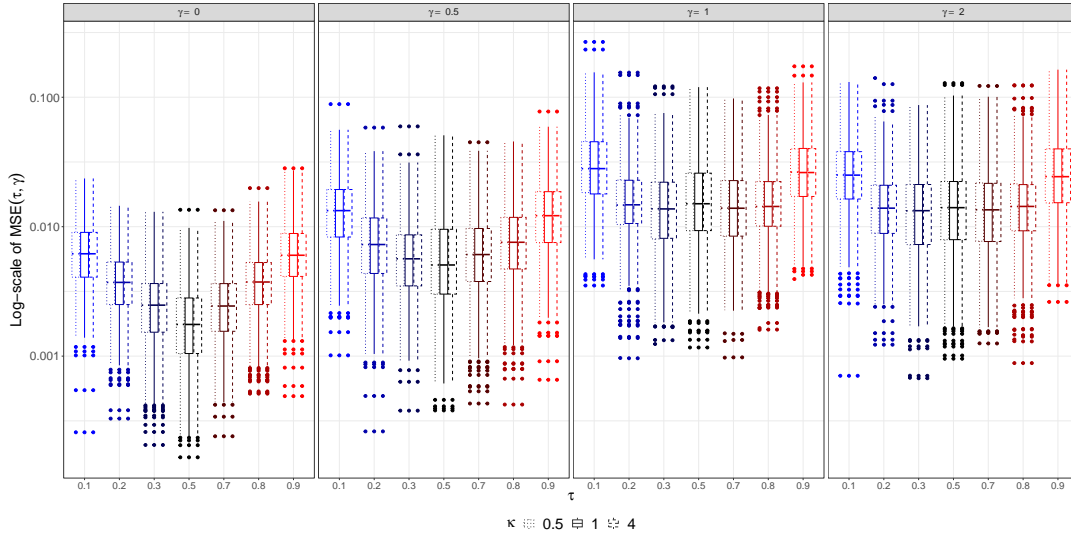


FIG 10. MSE values on the log-scale for four different simulation studies characterized by different values of  $\gamma$  (from left to right panel by increasing magnitude), and estimated with three different values of  $\kappa$ . For each of them, we show the boxplots for different extremile levels, namely  $\tau = 0.1, 0.2, 0.3, 0.5, 0.7, 0.8, 0.9$ .

As far as the application goes, Figures 11 and 12 show the average temperature and wind speed profiles in the month of July with the corresponding shifts, respectively, namely

$$\begin{aligned} AvgTemp_7(s) + \Delta_j^{(Temp)}, \quad j = 1, \dots, 31, s \in \mathcal{S}, \\ AvgWind_7(s) + \Delta_j^{(Wind)}, \quad j = 1, \dots, 31, s \in \mathcal{S}. \end{aligned}$$

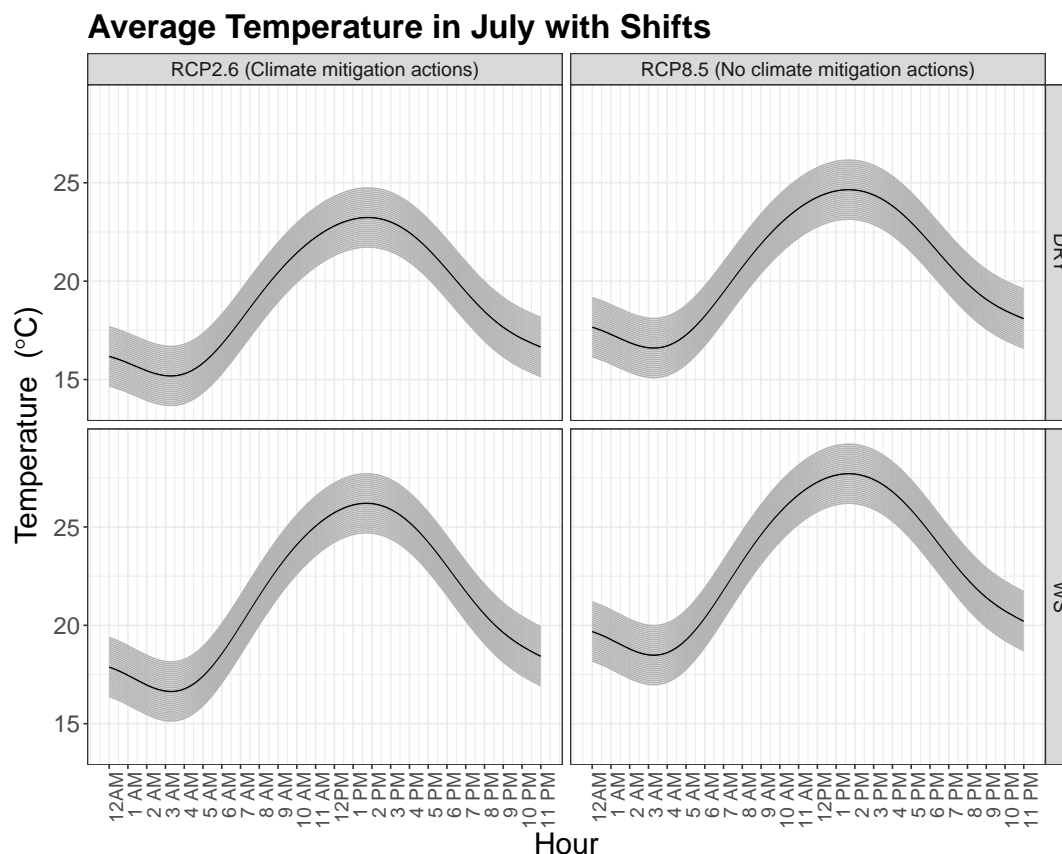


FIG 11. Average temperature in the month of July in the two scenarios, RCP2.6 (first column) and RCP8.5 (second column), for both reference year (first row) and warm summer (second row) cases.

## REFERENCES

- BAÍLLO, A. and GRANÉ, A. (2009). Local linear regression for functional predictor and scalar response. *Journal of Multivariate Analysis* **100** 102-111. <https://doi.org/10.1016/j.jmva.2008.03.008>
- BATTAGLIOLA, M. L. (2024). LauraBattagliola/ExtrFunReg: ExtrFunReg package. <https://doi.org/10.5281/zenodo.11400425>
- BATTAGLIOLA, M. L., SØRENSEN, H., TOLVER, A. and STAIUCU, A.-M. (2024). Quantile Regression for Longitudinal Functional Data with Application to Feed Intake of Lactating Sows. *Journal of Agricultural, Biological and Environmental Statistics*. <https://doi.org/10.1007/s13253-024-00601-5>
- BELLINI, F., KLAR, B., MÜLLER, A. and ROSAZZA GIANIN, E. (2014). Generalized quantiles as risk measures. *Insurance: Mathematics and Economics* **54** 41-48. <https://doi.org/10.1016/j.insmatheco.2013.10.015>
- DI BERNARDINO, E., LALOË, T. and PAKZAD, C. (2024). Estimation of extreme multivariate expectiles with functional covariates. *Journal of Multivariate Analysis* **202** 105292. <https://doi.org/10.1016/j.jmva.2023.105292>
- BEYAZTAS, U., SHANG, H. L. and ALIN, A. (2022). Function-on-Function Partial Quantile Regression. *Journal of Agricultural, Biological and Environmental Statistics* **27** 149-174. <https://doi.org/10.1007/s13253-021-00477-9>
- BLADT, M., ALBRECHER, H. and BEIRLANT, J. (2020). Threshold selection and trimming in extremes. *Extremes* **23** 629-665. <https://doi.org/10.1007/s10687-020-00385-0>
- BOJ, E., DELICADO, P. and FORTIANA, J. (2010). Distance-based local linear regression for functional predictors. *Computational Statistics & Data Analysis* **54** 429-437. <https://doi.org/10.1016/j.csda.2009.09.010>
- BONNER, S. J., NEWLANDS, N. K. and HECKMAN, N. E. (2014). Modeling regional impacts of climate teleconnections using functional data analysis. *Environmental and ecological statistics* **21** 1-26. <https://doi.org/10.1007/s10651-013-0241-8>
- CH2018 (2018). Climate scenarios for Switzerland Technical Report, National Centre for Climate Services. ISBN: 978-3-9525031-4-0.

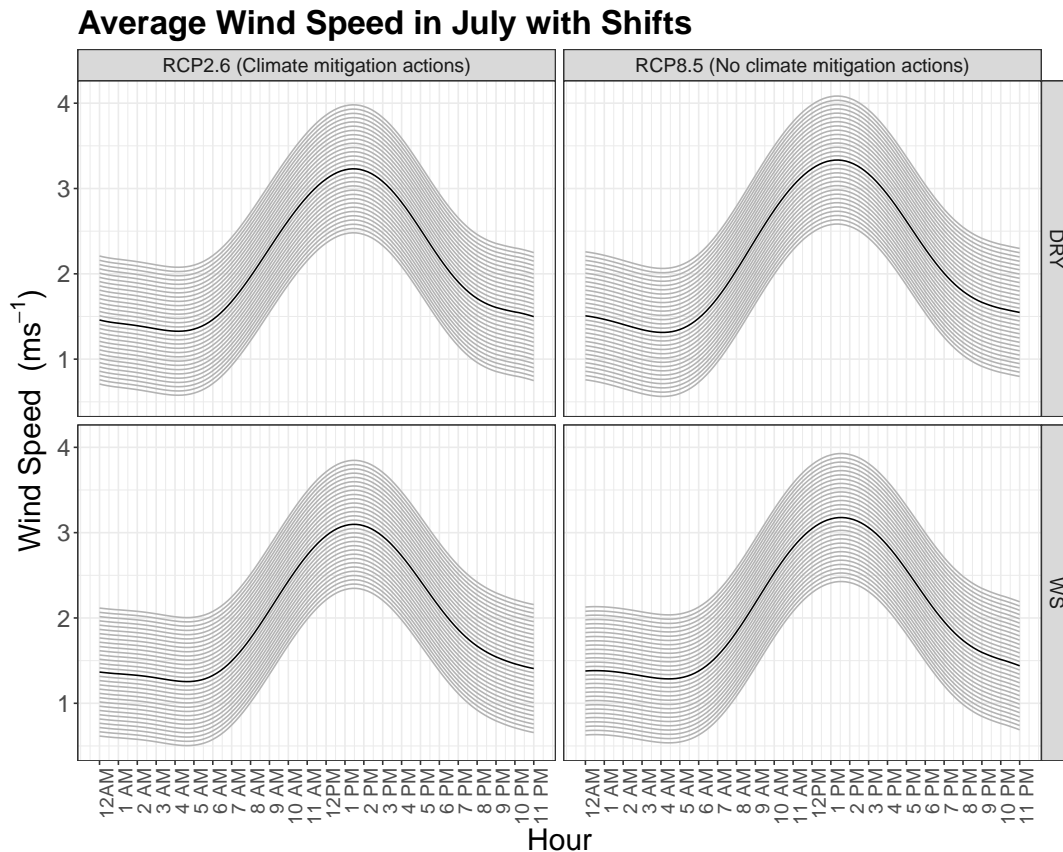


FIG 12. Average wind speed in the month of July in the two scenarios, RCP2.6 (first column) and RCP8.5 (second column), for both reference year (first row) and warm summer (second row) cases.

- CHAGNY, G. and ROCHE, A. (2014). Adaptive and minimax estimation of the cumulative distribution function given a functional covariate. *Electronic Journal of Statistics* **8** 2352 – 2404. <https://doi.org/10.1214/14-EJS956>
- DAOUIA, A., GIJBELS, I. and STUPFLER, G. (2019). Extremiles: A New Perspective on Asymmetric Least Squares. *Journal of the American Statistical Association* **114** 1366–1381. <https://doi.org/10.1080/01621459.2018.1498348>
- DAOUIA, A., GIJBELS, I. and STUPFLER, G. (2022). Extremile regression. *Journal of the American Statistical Association* **117** 1579–1586. <https://doi.org/10.1080/01621459.2021.1875837>
- FASIOLO, M., WOOD, S. N., ZAFFRAN, M., NEDELLEC, R. and GOUDE, Y. (2021). qgam: Bayesian Nonparametric Quantile Regression Modeling in R. *Journal of Statistical Software* **100** 1–31. <https://doi.org/10.18637/jss.v100.i09>
- FERRATY, F. and NAGY, S. (2021). Scalar-on-function local linear regression and beyond. *Biometrika* **109** 439–455. <https://doi.org/10.1093/biomet/asab027>
- FERRATY, F. and VIEU, P. (2006). *Nonparametric Functional Data Analysis: Theory and Practice (Springer Series in Statistics)*. Springer-Verlag, Berlin, Heidelberg. <https://doi.org/10.1007/0-387-36620-2>
- FERRATY, F., LAKSACI, A., TADJ, A. and VIEU, P. (2010). Rate of uniform consistency for nonparametric estimates with functional variables. *Journal of Statistical Planning and Inference* **140** 335–352. <https://doi.org/10.1016/j.jspi.2009.07.019>
- FISCHER, A. M., STRASSMANN, K. M., CROCI-MASPOLI, M., HAMA, A. M., KNUTTI, R., KOTLARSKI, S., SCHÄR, C., SCHNADT POBERAJ, C., BAN, N., BAVAY, M., BEYERLE, U., BRESCH, D. N., BRÖNNIMANN, S., BURLANDO, P., CASANUEVA, A., FATICHI, S., FEIGENWINTER, I., FISCHER, E. M., HIRSCHI, M., LINIGER, M. A., MARTY, C., MEDHAUG, I., PELEG, N., PICKL, M., RAIBLE, C. C., RAJCZAK, J., RÖSSLER, O., SCHERRER, S. C., SCHWIERZ, C., SENEVIRATNE, S. I., SKELTON, M., SØRLAND, S. L., SPIRIG, C., TSCHURR, F., ZEDER, J. and ZUBLER, E. M. (2022). Climate Scenarios for Switzerland CH2018 – Approach and Implications. *Climate Services* **26** 100288. <https://doi.org/10.1016/j.cliser.2022.100288>
- FRAIMAN, R., JUSTEL, A., LIU, R. and LLOP, P. (2014). Detecting trends in time series of functional data: A study of Antarctic climate change. *Canadian Journal of Statistics* **42** 597–609. <https://doi.org/10.1002/cjs.11231>

- GARDES, L. and GIRARD, S. (2012). Functional kernel estimators of large conditional quantiles. *Electronic Journal of Statistics* **6** 1715 – 1744. <https://doi.org/10.1214/12-EJS727>
- GIRARD, S., STUPFLER, G. and USSEGLIO-CARLEVE, A. (2022). Functional estimation of extreme conditional expectiles. *Econometrics and Statistics* **21** 131–158. <https://doi.org/10.1016/j.ecosta.2021.05.006>
- GUO, M., ZHOU, L., HUANG, J. Z. and HÄRDLE, W. K. (2015). Functional data analysis of generalized regression quantiles. *Statistics and Computing* **25** 189–202. <https://doi.org/10.1007/s11222-013-9425-1>
- J. BARRIENTOS-MARIN, F. F. and VIEU, P. (2010). Locally modelled regression and functional data. *Journal of Nonparametric Statistics* **22** 617–632. <https://doi.org/10.1080/10485250903089930>
- JONES, M. C. (1994). Expectiles and M-quantiles are quantiles. *Statistics & Probability Letters* **20** 149–153. [https://doi.org/10.1016/0167-7152\(94\)90031-0](https://doi.org/10.1016/0167-7152(94)90031-0)
- KOENKER, R. and BASSETT, G. (1978). Regression Quantiles. *Econometrica* **46** 33–50. <https://doi.org/10.2307/1913643>
- LI, M., WANG, K., MAITY, A. and STAIU, A.-M. (2022). Inference in functional linear quantile regression. *Journal of Multivariate Analysis* **190** 104985. <https://doi.org/10.1016/j.jmva.2022.104985>
- MOHAMMEDI, M., BOUZEZBA, S. and LAKSACI, A. (2021). The consistency and asymptotic normality of the kernel type expectile regression estimator for functional data. *Journal of Multivariate Analysis* **181** 104673. <https://doi.org/10.1016/j.jmva.2020.104673>
- NEWBY, W. K. and POWELL, J. L. (1987). Asymmetric Least Squares Estimation and Testing. *Econometrica* **55** 819–847. <https://doi.org/10.2307/1911031>
- RACHDI, M., LAKSACI, A. and AL-KANDARI, N. M. Expectile regression for spatial functional data analysis (sFDA). *Metrika*. <https://doi.org/10.1007/s00184-021-00846-x>
- CH2018 PROJECT TEAM (2018). CH2018 - Climate Scenarios for Switzerland. <https://doi.org/10.18751/Climate/Scenarios/CH2018/1.0>
- SØRLAND, S. L., FISCHER, A. M., KOTLARSKI, S., KÜNSCH, H. R., LINIGER, M. A., RAJCZAK, J., SCHÄR, C., SPIRIG, C., STRASSMANN, K. and KNUTTI, R. (2020). CH2018 – National climate scenarios for Switzerland: How to construct consistent multi-model projections from ensembles of opportunity. *Climate Services* **20** 100196. <https://doi.org/10.1016/j.cliser.2020.100196>
- SUHAILA, J. and YUSOP, Z. (2017). Spatial and temporal variabilities of rainfall data using functional data analysis. *Theoretical and Applied Climatology* **129** 229–242. <https://doi.org/10.1007/s00704-016-1778-x>
- TAPIA, M., HEINEMANN, D., BALLARI, D. and ZONDERVAN, E. (2022). Spatio-temporal characterization of long-term solar resource using spatial functional data analysis: Understanding the variability and complementarity of global horizontal irradiance in Ecuador. *Renewable Energy* **189** 1176–1193. <https://doi.org/10.1016/j.renene.2022.03.049>
- R CORE TEAM (2023). R: A Language and Environment for Statistical Computing R Foundation for Statistical Computing, Vienna, Austria.
- VILLANI, V., ROMANO, E. and MATEU, J. (2024). Climate model selection via conformal clustering of spatial functional data. *Environmental and Ecological Statistics*. <https://doi.org/10.1007/s10651-024-00616-8>
- YU, D., KONG, L. and MIZERA, I. (2016). Partial functional linear quantile regression for neuroimaging data analysis. *Neurocomputing* **195** 74–87. <https://doi.org/10.1016/j.neucom.2015.08.116>
- ZHANG, X., SHAO, X., HAYHOE, K. and WUEBBLES, D. J. (2011). Testing the structural stability of temporally dependent functional observations and application to climate projections. *Electronic Journal of Statistics* **5** 1765 – 1796. <https://doi.org/10.1214/11-EJS655>